IJCRT.ORG ISSN : 2320-2882

INTERNATIONAL JOURNAL OF CREATIVE RESEARCH THOUGHTS (IJCRT)

An International Open Access, Peer-reviewed, Refereed Journal

ZNO BASED ULTRAVIOLET (UV) PHOTO-TRANSISTOR WITH PLASMONIC ENHANCEMENT

SHIVESH KUMAR, DHARMENDRA KUMAR, DR. AMRITANSHU PANDEY
RESEARCH SCHOLAR, RESEARCH SCHOLAR, ASSOCIATE PROFESSOR
IIT BHU(VARANASI)

ABSTRACT

Nanostructured material has drawn huge attention due to their attractive photo detection properties. Compare with other materials ZnO has much importance in the device fabrication purpose due to its direct wide band gap of ~ 3.3ev, large excitation binding energy of ~ 60mv at room temperature and high electron mobility. Many works have been reported that use ZnO for the purpose of UV photodetectors.

This thesis presents the simulation studies of ZnO based Ultraviolet (UV) Photo-Transistor with and without plasmonic. By using plasmonics the output current increase by a factor of 100, It also improve the source photo current and sensitivity. The simulations were carried out using ATLAS software. The material used in this project is ZnO with a doping concentration of $10^{17}/cm^3$.The plasmonic layer was of platinum nanoparticles.

The photodetector was irradiated with intensity of 550 mW/cm^2 UV radiation of wavelength 350nm. The output currents of ZnO based UV Photo-Transistors with and without plasmonic layer were found to be 1.2755×10^{-5}A and 3.048×10^{-7}A respectively. And the maximum responsivity of the devices was found to be 0.0654mA/W and 0.18μA/W with and without plasmonic layer; respectively it was also observed that there is an appreciable increase (factor of 100) in source photo current in devices with a plasmonic layer.

CONTENTS

LIST OF FIGURES

Figure **Page No.**

LIST OF TABLES

CHAPTER 1

1 INTRODUCTION

1.1 Introduction

Nanotechnology manipulates matter at the atomic, molecular or macromolecular level to create and control objects on the nanometer scale, with the goal of fabricating novel materials, devices and systems that have new properties and functions because of their small size. Nanoscale materials are those where at least one of their characteristic dimensions lie between approximately 1 and 100 nanometers (nm).

Within this length scale, the characteristics of the matter could become significantly different from individual atoms or molecules and from their bulk counterparts. Thus, their study has recently been recognized as a novel area of science, and is generally termed 'Nanoscience'. However, even more popular is the term 'Nanotechnology', which signifies the construction of functional devices based on the controlled assembly of nanoscale objects for specific technological applications.

The significance of this relatively new area of study is exemplified by a number of national and international initiatives promoting its research. Funding agencies are devoting a major part of their funding for nanotechnology, and likewise the amount of research that is performed in this field has dramatically increased during the past couple of decades.

Nanoparticles (NPs), particles with dimensions between 1 to l00nm, are probably the most researched materials within the field of nanotechnology, and they exhibit unique electronic, optical, photonic and catalytic properties [1-2]. Tremendous scientific progress has been made in the past few years in the synthesis, characterization and functionalization of such nanoparticles.

1.2 UV Photodetectors

Photo detection in the ultraviolet (UV) region has drawn extensive attention owing to its various applications in industry, instrument, and our daily life. UV light is typically divided into four spectral regions: UV-A (for

wavelengths between 400 and 320 nm), UV-B (for wavelengths between 320 and 280 nm), UV-C (for wavelengths between 280 and 200 nm), and far UV (for wavelength between 200 and 10 nm) [3–5]

The detection of UV radiation presents a wide range of applications, such as chemical, environmental and biological analysis or monitoring, flame and radiation detection, astronomical studies, and optical communications.

An ultraviolet (UV) photodetector exhibiting enhanced response characteristics has been realized successfully after integrating various metal nanoparticles (NPs) such as silver (Ag), gold (Au) and platinum (P_t) with sol–gel derived ZnO thin film (NPs–ZnO). The metal NP based photodetector (Ag, Au, P_t-NPs-ZnO) exhibits a relatively high photo response in comparison to the bare ZnO based UV photodetector and gives a maximum value of about 4.27×10^3.

The combined effect of the lowering of dark current due to the formation of a Schottky barrier at the interface of the metal NPs with the ZnO thin film and the photocurrent upon UV illumination due to the plasmonic effect of loaded NPs results in an enhanced photo response of the prepared metal NP–ZnO photodetector. The trapping of incident UV radiation mainly through the enhanced optical absorption by loaded metal NPs due to the plasmonic effect and subsequent coupling of harvesting photons into underlying optical modes of the surface of photo conducting ZnO thin films lead to a significant increase in photo current.

1.3 Effect of Plasmon on Transistor

One of the key functions for the use of the plasmonic effect is an efficient conversion of Plasmon energy to an electrical signal or vice versa. A metal−semiconductor junction structure enables plasmonic energy detection as a form of electrical current [6-10]. Plasmonic energy is proportional to the square root of the density (n) of valence electrons (approximately equal to free-electron density).

$$E_{plasmon} = \hbar\sqrt{\frac{n_e^2}{\epsilon_0 m_e}} \quad \hbar\sqrt{\frac{n_e^2}{\epsilon_0 m_e}}$$

Where,

ħ - The reduced Planck constant.

e - The charge of the electron.

m_e - The effective mass of the electron.

ε_o - The permittivity of vacuum (or called the dielectric constant of free space)

Typical values of the Plasmon energies of materials are between 5eV and 30eV. Photons absorbed in a metal nanostructure generate hot electrons and the electrons can cross by thermionic diffusion at the boundary between metal and semiconductor which produce photocurrent. The Plasmon transistor collects plasmonically induced hot electrons from the metal nanostructures, and these hot electrons contribute to the amplification of the drain current by modulating the channel conductivity. Moreover, the gate voltage bias controlled internal electric field and quantum tunneling effect at the metal−semiconductor junction enable efficient hot electron collection and amplification. On the basis of the work function difference between platinum and n-type ZnO, it is expected that a Schottky barrier is formed with around 1.3−1.4 eV of barrier height. Thus, the generated hot electrons with higher energy than this Schottky barrier can thermionically diffuse from platinum NPs to the ZnO layer. The figure 1.1 shown the plasmonic Field Effect Transistor structure in which a heavily doped n-type S_i substrate serves as a back gate and an n-type ZnO film deposited on thermally grown sio_2 serves as an active semiconductor channel.

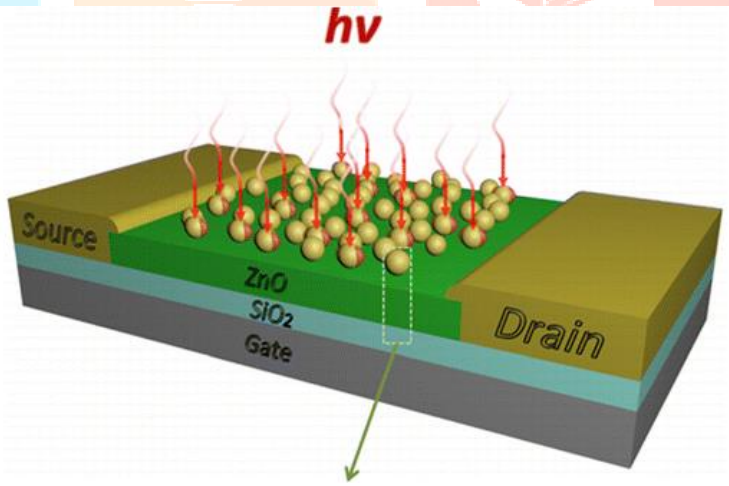

igure 1.1 Illustration of Plasmon FET structure and operational principle of Plasmon FET under light illumination

As discussed earlier, the plasmonic absorption generates hot electrons in platinum NPs and these energetic hot electrons can migrate across the Schottky barrier and diffuse to the ZnO film (Figure1.1) Consequently, this process supplies more electrons in the ZnO channel, resulting in increased channel conductivity and drain current (I_d). Because the number of migrated hot electrons depends on the plasmonic absorption of platinum NPs, the expected

drain current response as a function of wavelength should be matched with the absorption spectrum of platinum NPs. Therefore, the Plasmon−Field Effect Transistor converts localized surface Plasmon energy to electrical charges and their flow. Furthermore, Plasmon energy was amplified with gate voltage bias, facilitating quantum tunneling of electrons from gold NPs into the ZnO channel.

1.4 ZnO based Photo-Transistors

A phototransistor is identical to a Thin Film Transistor in device structure, with the channel layer acting as an optically active area. Compared to the traditional UV PDs, the phototransistor has a gigantic responsivity as the drain current (I_D) can be amplified by controlling the gate voltage (Vg). The response time is dominated by the on/off time of the phototransistor, which can be used to erase the persistent photocurrent (PPC) effect.

Thin Film Transistor is a type of Field Effect Transistor (FET) that controls current flow between source and drain contacts by the voltage applied to the gate electrode. The voltage gives rise to an electric field in the semiconductor that attracts, accumulate, and charge. These create a channel for charges and let them more easily move between source and drain current. A Thin Film Transistor is a field-effect transistor (FET) having three terminals (gate, source, and drain) and including semiconductor, dielectric, and conductive layers, which are shown in (figure 1.2). For making the device we use ATLAS software. The semiconductor is placed between source/drain electrodes and the dielectric is located between the gate electrode and the semiconductor. The main idea in this device is to control the current between drain and source (I_{DS}) by varying the potential between gate and source (V_{GS}), inducing free charge accumulation at the dielectric/semiconductor interface [11].

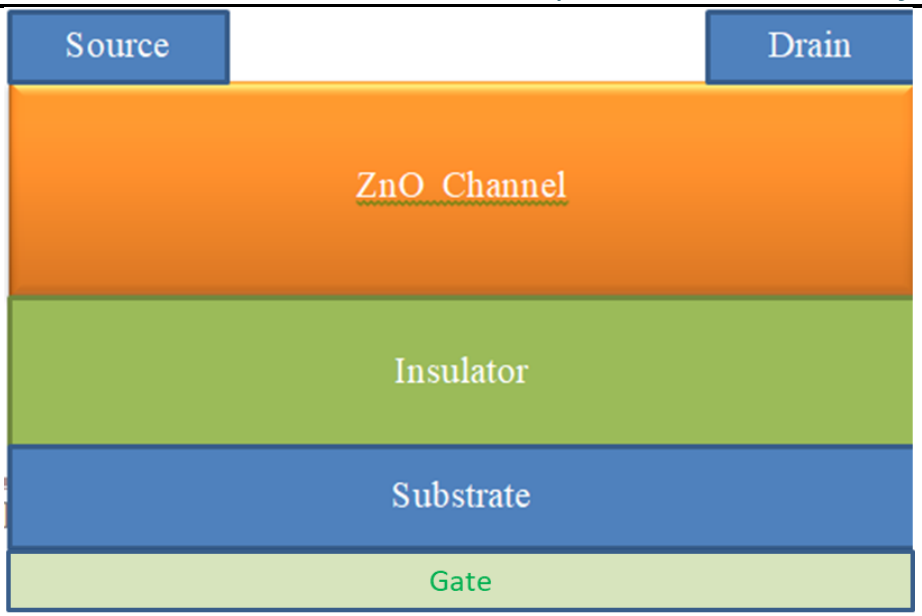

Figure 1-1 ZnO Channel thin film transistor design.

We perform the electrical behavior of the device by measuring the threshold voltage V_{th} in volts, Ion/off, field effect mobility in cm^2/v-s, which is explained below:

4.1 Threshold Voltage

Threshold voltage (V_T) is defined as the applied gate voltage at which the channel of mobile carriers begins to form and thus the TFT devices begin to switch from 'off' to 'on'. The importance of (V_T) is that it helps to determine the necessary supply voltage for circuit operation. The value of threshold voltage is commonly extracted from the following two methods. The first method extracts V_T from the transfer curve of a TFT in the linear region of operation when a small V_{DS} is applied, the simplified equation is given below

$$I_{ds} = \frac{1}{2}\mu_n C_{ox}\frac{w}{l}\left[(V_{GS} - V_T)V_{DS}\right] \quad \ldots\ldots\ldots\ldots\ldots\ldots\ldots\ldots\ldots\ldots (1)$$

Another meth fer curve of TFT in the saturation region of operation,

The drain cur v model of Thin Film Transistor is given by [8-9] in equation (2).

$$I_{DS} = \frac{1}{2}\mu_n C_{ox}\frac{w}{l}(V_{GS} - V_{th})^2 \quad \ldots\ldots\ldots\ldots\ldots\ldots\ldots\ldots\ldots\ldots\ldots\ldots\ldots\ldots (2)$$

Where, W, L, C_G and μ are the TFT channel width, length, and gate capacitance and field-effect mobility respectively.

1.4.2 On/Off current ratio

Drain current on/off ratio is another measure of the switching behavior of the TFT. It is simply the ratio between highest measured current (the on-state current, Ion) to the lowest measured current (the off-state current, I_{off}). I_{off} is also a measure of the gate leakage present in the device.

1.4.3 Field Effect Mobility

Mobility (μ) is a material property that is used to describe the drift velocity of electrons or holes to the applied electric field across a material. The most widely used term for mobility is field-effect mobility which represents the mobility of carriers under the influence of the device structure in field-effect transistors.

Mobility is a proportionality constant which relates the drift velocity to the applied electric field. To estimate the carrier mobility the two commonly used definitions are effective mobility and field-effect mobility, extracted from the drain conductance dI_d/dV_{ds} in linear region and trans conductance (d_{IDS}/d_{VDS}) gm of transfer characteristics, respectively.

1.5 Semiconductor Photodetectors

A semiconductor photodetector is an optoelectronic device that converts the incident optical signal to an electrical signal or which convert light into some other types of energy, such as thermal or electrical energy. Photoelectric effect is the principle applies to photodetector which is effect on a circuit due to light. The photoelectric effect is the effect of light on a surface of metal in a vacuum, the result is electronics being ejected from the surface this explains the principle theory of light energy that allows photodetector to operate.

Max Planck in 1900 discovered that energy is radiated in small discrete units called quanta; he also discovered a universal constant of nature which is known as the Planck's constant. These discoveries lead to a new form of physics known as quantum mechanics and the photoelectric effect $E=h\upsilon$ which is frequency of radiation multiplied by the Planck's constant. The modern applications of photodetectors are numerous and they are important for fiber optics, Photography, astronomy, spectroscopy, plasma physics, Sensors and monitoring.

5.1 Working Principle of Photodetector

The working principle of a semiconductor photodetector (i.e. photo detection mechanism) can be divided into two main steps:

) absorption of photons by a semiconductor and electron hole pair generation

i) Drift of these charge carriers with an electric field and collection of drifted charge carriers.

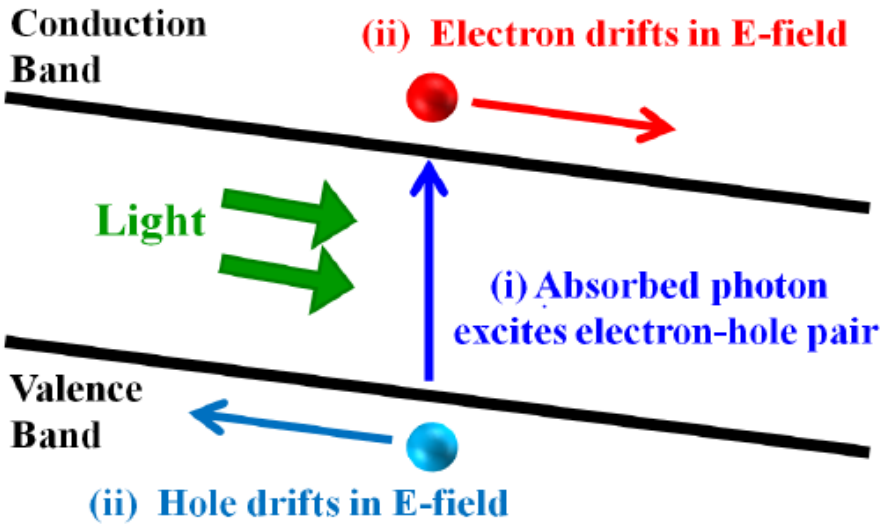

Figure 1-2 Photo detection process in the semiconductor photodetectors

The above figure shows the photo detection process of semiconductor photodetector. For the absorption of an incident photon, it should have sufficient energy to excite an electron from one state to another inside the semiconductor. Typically, this excitation occurs from valence band to conduction band of semiconductor and it is called intrinsic or band-to-band absorption as shown in (figure 1.3(i)). The intrinsic transition requires a photon with a minimum energy equals to the band gap of the semiconductor. In semiconductors with crystallographic defects, which act as donor or acceptor defect states in the forbidden band gap, there is also a sub-band gap absorption mechanism. This mechanism is coined as extrinsic absorption mechanism which is the excitation of an electron (ii) from the valence band to a defect state or (iii) from a defect state to the valence band, all are shown in (figure 1.3), which is shown below:

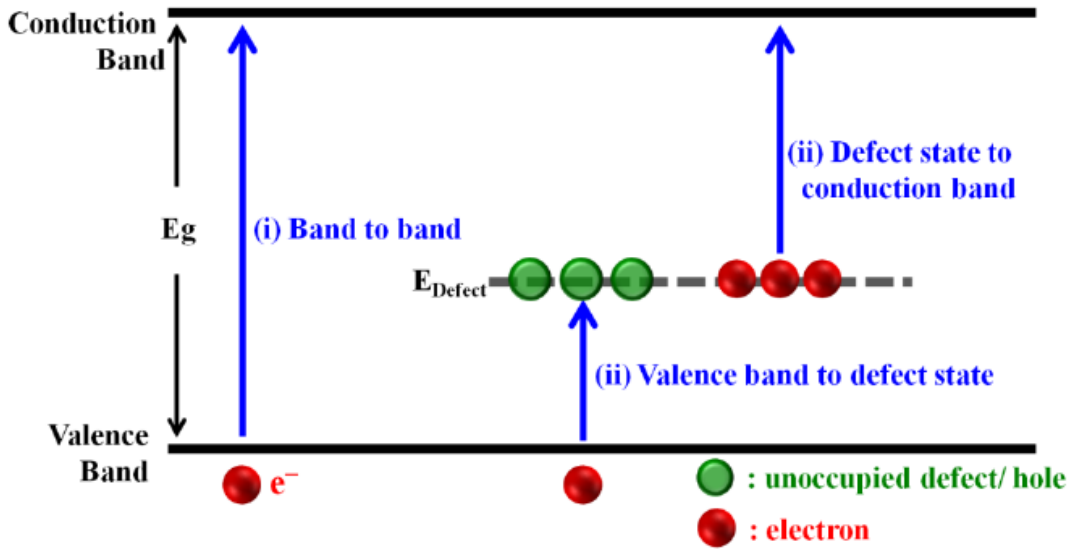

Figure 1-3 Photoexcitation mechanisms: (i) from valence band to conduction band, (ii) from valence band to defect state, and (iii) from defect state to conduction band.

After the generation of charge-carrier (i.e. electron-hole) pair, the electric field in the semiconductor pushes electron and hole away from each other. The photodiodes have an either p-n, p-i-n or Schottky junction to generate a built-in electric field which would separate charges. On the other hand, in photoconductors, an external bias is applied to create an electric field in the semiconductor and separate the charges. When the photo generated electrons and holes are separated in the semiconductor, the electric field drifts them towards anode and cathode contacts which complete the photo detection process.

5.2 Photoconductors

The semiconductor photodetectors can be separated as photodiodes and photoconductors in terms of having a junction and built-in potential. The photodiodes have a junction (i.e. p-n, p-i-n or Schottky) to separate and collect the photo generated charges. They are commonly used in industrial applications due to their high performance and low cost. On the contrary, the photoconductors do not have such a junction and they are based on photoconductivity, which is the variation of conductivity of a semiconductor when it is exposed to light. When it is compared with photodiodes, it is easy to fabricate a photoconductor which is simply a slab of semiconductor with two ohmic contacts. The semiconductor in photoconductors is usually deposited with relatively simple processes like thermal evaporation and sputtering.

1.5.3 (a) Schottky contact

The formation of Schottky Barrier (SB) between a semiconductor and metal is widely utilized in semiconductor devices. A Schottky barrier refers to a metal-semiconductor contact having a large barrier height (i.e. ϕ_B>KT) and low doping concentration that is less than the density of states in the conduction band or valence band. The potential barrier between the metal and the semiconductor can be identified on an energy band diagram. The local Schottky Barrier height is found to vary between 0 to 1.26eV depending on the position of the dopant.

To construct such a diagram we first consider the energy band diagram of the metal and the semiconductor, and align them using the same vacuum level as shown in Figure 1-4(a) as the metal and semiconductor are brought together, the Fermi energies of the two materials must be equal at thermal equilibrium shown in figure 1-4(b).

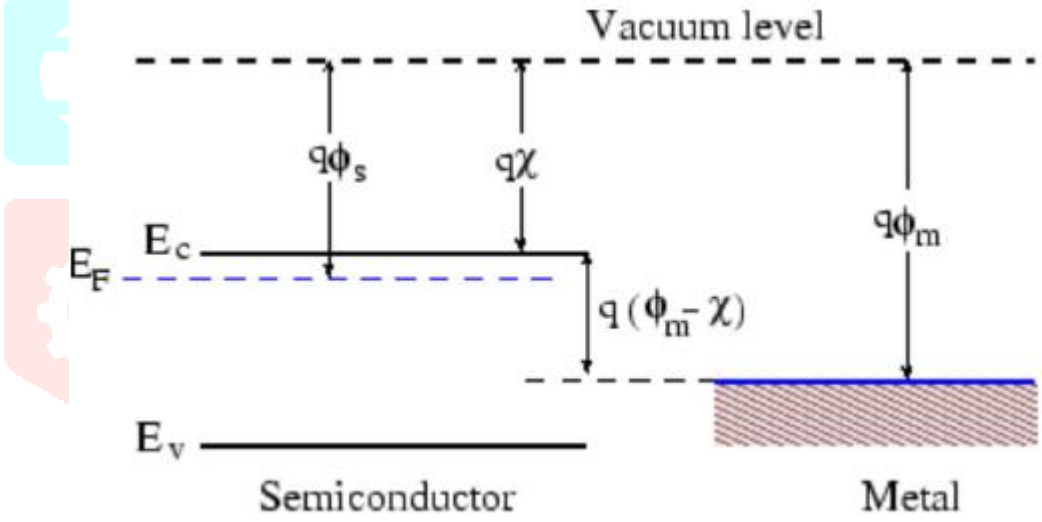

Figure 1-4(a) Energy band diagram of metal-semiconductor contact in thermal non-equilibrium

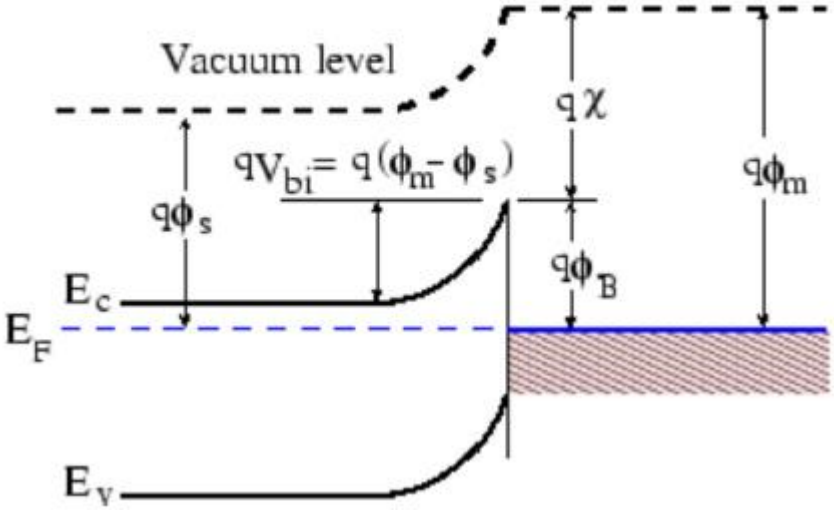

Figure1-4(b) Energy band diagram of metal-semiconductor contact in thermal equilibrium

In the given figure the barrier height ϕ_B is defined as the potential difference between the Fermi energy of the metal and the band edge where the majority carrier reside from (figure 1-4(b)), one finds that for n-type semiconductors the barrier height is obtained from the given equation

$$\phi_{Bn} = \phi_m - \chi \qquad \ldots\ldots\ldots\ldots\ldots\ldots\ldots\ldots\ldots\ldots\ldots\ldots\ldots\ldots\ldots\ldots\ldots\ldots(3)$$

Where ϕm is the work function of the metal and χ is the electron affinity. The work function of selected metals as measured in vacuum can be found in (figure 1-5).

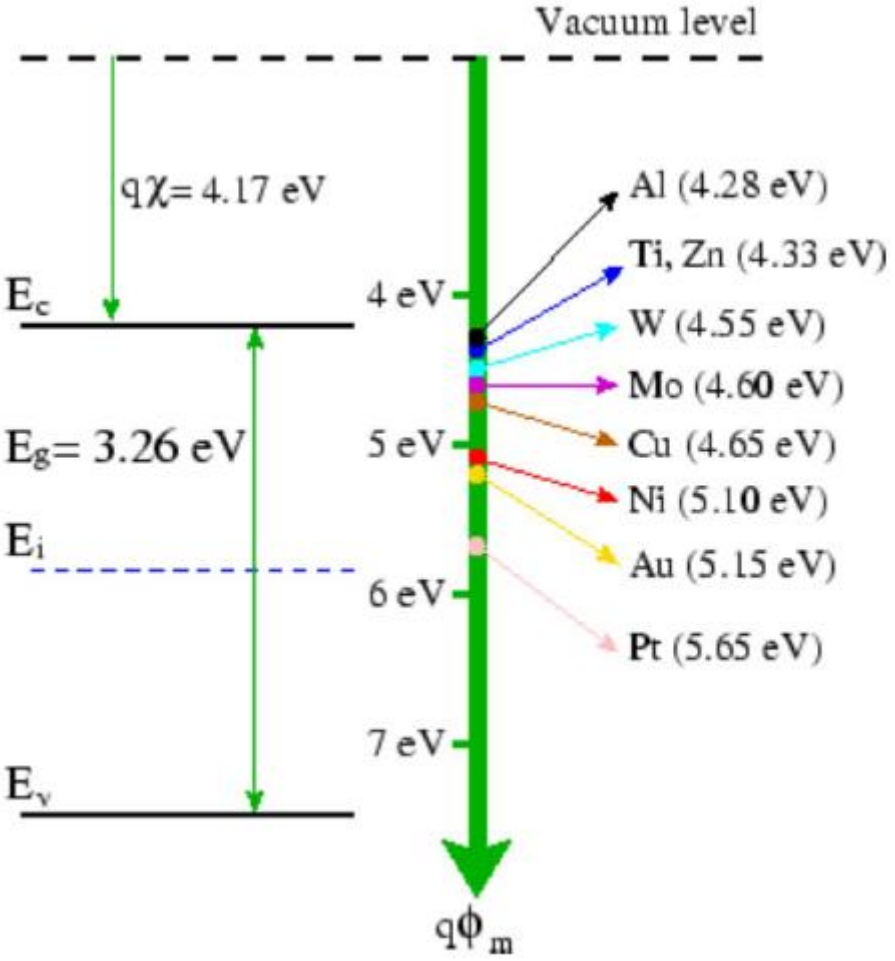

Figure 1-5 Energy band diagrams of the selected metals

For p-type material, the barrier height is given by the difference between the valence band edge and the Fermi energy in the metal, which are shown below

$$\phi_{Bp} = \frac{E_g}{q} + \chi - \phi_m \quad \text{..... (4)}$$

A metal-semiconductor junction will therefore form a barrier for electrons and holes, if the Fermi energy of the metal is located between the conduction and the valence band edge.

For N-type material the work function difference as the difference between the work function of the metal and that of the semiconductor as shown below:

$$\phi_{wf} = \phi_m - \chi - \frac{E_{c-E_{F,n}}}{q} \quad \text{..... (5)}$$

Similarly for P-type material

$$\phi_{wf} = \chi + \frac{E_{c-E_{F,p}}}{q} - \phi_m \quad \text{..... (6)}$$

Hence the work function difference energy becomes:

$$E_w = q.\ \phi_{wf} \quad \text{..... (7)}$$

The measured barrier height for selected metal junction is listed in Table1.1

Table 1-1Work function of selected metal and there barrier height

	Al	Ti	Zn	W	Mo	Cu	Ni	Au	Pt
ϕ_m	4.28	4.33	4.33	4.55	4.60	4.65	5.10	5.15	5.65
ϕ_B	1.01	1.06	1.06	1.28	1.33	1.38	1.63	1.68	2.08

1.5.3 (b) Ohmic contact

An ohmic contact is defined as a metal-semiconductor contact that has a negligible contact resistance relative to the bulk or series resistance of the semiconductor. A satisfactory ohmic contact should not significantly degrade device performance and can pass the required current with a voltage drop that is small compared with the drop across the active region of the device. The metal quasi-FERMI level (which is specified by the contact voltage) is equal to the semiconductor quasi-FERMI level. The contact potential ϕ_s at the semiconductor boundary is given as:

..... (8)

Where, Ψ_{bi} is the b

$$\phi_s = \phi_m + \Psi_{bi}$$

1.5.4 Types of Photodetectors

There are many type of photodetector which are used in many photonics application. The use of photodetector is to calculate optical power or energy.

1.5.4.1 Photodiodes

Photodiodes are semiconductor devices with a p–n junction or p–i–n structure (i = intrinsic material) (→ p–i–n photodiodes), where light is absorbed in a depletion region and generates a photocurrent. Such devices can be very compact, fast, highly linear, and exhibit a high quantum efficiency (i.e., generate nearly one electron per incident photon) and a high dynamic range, provided that they are operated in combination with suitable electronics.

1.5.4.2 Metal-Semiconductor-Metal Photodetectors

It contains two Schottky contacts instead of a p–n junction. They are potentially faster than photodiodes, with bandwidths up to hundreds of gigahertz. Metal-semiconductor-metal photodetectors are generally known as high-speed photodetectors and have valuable uses in the fields of communications, research and photograph.

A metal-semiconductor-metal photodetector is a flat (planar) structure which has several layers. The "base" layer is a semiconductor layer which absorbs photons from a light source. Onto this layer are deposited metal electrodes. The electrodes are "interdigitated", or alternating, and form Schottky contacts.

A Schottky contact is generically defined as a contact point between a metal and a semiconductor, Transmitted information is detected when incident light is absorbed by the semiconductor medium and the electron-hole pairs created are collected by the external circuit.

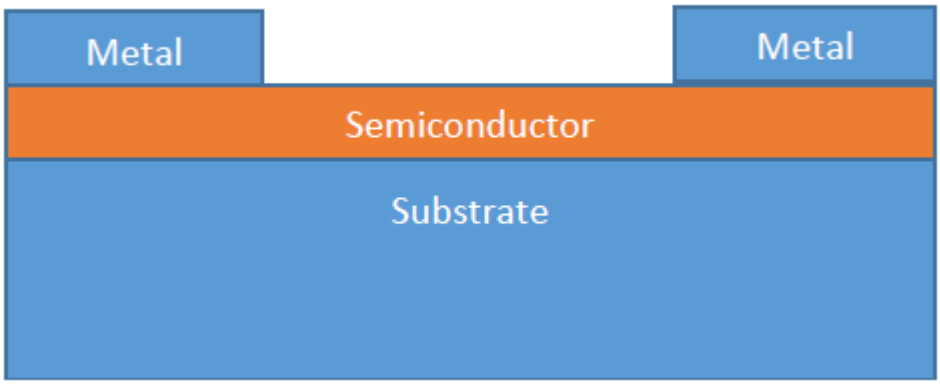

Figure 1-6 Schematic of MSM detectors

A conventional metal-semiconductor-metal photodetector is shown in figure 1.4. A semi-insulating base or substrate physically supports the structure and insulates the electrodes from each other and their surroundings. The active layer semiconductor is the area where photonic conversion to electrons and holes occurs. Metal electrodes are deposited onto the surface, and alternate between electrodes in an interdigitated manner [12].

1.5.4.3 Photo resistors

Photo resistors are also based on certain semiconductors, e.g. cadmium sulfide (CdS). They are cheaper than photodiodes, but they are fairly slow, are not very sensitive, and exhibit a strongly nonlinear response.

1.5.4.4 Thermal Detectors

A thermal detector absorbs radiation and changes temperature. Because the power in absorbed radiation is typically rather small (10^{-7}W), the detector itself should be small so that it has a low heat capacity. Thermal detectors are of low manufacturing costs in comparison to photon detectors. The quality of these detectors was greatly improved after introduction of micromachining technology. Recently the uncooled arrays of these detectors working in the IR region (thermos vision cameras) are commercially available.

Thermal detectors (power meters) measure a temperature rise caused by the absorption of light. Such detectors can be very robust and be used for the measurement of very high laser powers, but exhibit a low sensitivity, moderate linearity, and relatively small dynamic range.

1.6 Parameters associated with Photodetectors

A photodetector's effectiveness is measured by its performance in many different parameters. These parameters include dark current, responsivity, speed, and spectral range. Dark current is generically defined as a current which flows in detectors when there is no radiant flux (light source) incident upon the electrodes.

6.1 Responsivity

Responsivity R_λ is defined as the ratio of radiant energy (in watts),p, incident on the photodiode to the photocurrent output in amperes I_p .It is expressed as as the absolute responsivity in amps per watt. Radiant energy is usually

expressed as w/cm^2 and that photodiode current as A/cm^2.Responsivity will vary with change in wavelength, bias voltage, and temperature. The responsivity of a photodetector is defined as:

$$R_\lambda = \frac{I_{ph}}{P_{opt}} = \eta\frac{q\lambda}{hc} \quad \text{..... (9)}$$

Where P_{opt} is the incident optical power

h is the plank constant=6.628×10^{-34} joule-sec

c is the velocity of light in air=3×10^8 m/s

And I_{ph} is the output photocurrent

6.2 Quantum Efficiency

It is defined as the fraction of incident photons which are absorbed by photoconductor and generated electrons which are collected at the detector terminal or we can say that Quantum efficiency is defined as fraction of incident photon which contributes to photocurrent.

Quantum efficiency is related to the responsivity as per following equation:

$$QE = R_\lambda \frac{1240}{\lambda} \quad \text{..... (10)}$$

Where: QE=Quantum efficiency in percent

R_λ=Responsivity of detector in A/W

λ=Wavelength in nanometer

6.3 Spectral Response

The spectral response is conceptually similar to the quantum efficiency and it is defined as the ratio of the current generated by the detector to the power incident on the detector .The ideal spectral response is limited at long wavelengths by the inability of the semiconductor to absorb photons with energies below the band gap. The spectral response decreases at small photon wavelength. At these wavelength, each photon has a large energy, and hence the ratio of photon to power is reduced .Any energy above the band gap energy is not utilized by the detector and

instead goes to heating the device. The inability to fully utilize the incident energy at high energies and the inability to absorb low energies of light represents a significant power loss in detectors consisting of a single p-n junction.

The relation between the quantum efficiency and spectral response is given as:

$$SR=\frac{q\lambda}{hc}(QE) \quad \text{..... (11)}$$

1.7 Objective of the work

In this dissertation, we simulate ZnO based Ultraviolet (UV) photo-transistor with plasmonic enhancement is proposed using two-dimensional device simulators using ATLAS Silvaco. ATLAS is a physically-based two and three dimensional device simulator that is used to estimate the electrical features which are related with quantified physical arrangement and bias settings. The main objective of the work is to improve the transient response, spectral response, Responsivity and photocurrent of the device. For this purpose we use 10nm platinum nanoparticles, which are kept on the devices and we found that there is appreciable increase (Factor of 100) in photo current. Hence we observed that plasmonic enhance the performance of the device

1.8 Organization of the thesis

This dissertation has six chapters, which includes first chapter as 'introduction' in which some general aspects of nanotechnology, photodetector and its application, introduction of ZnO based UV Photo Transistors are covered.

Chapter 2

This chapter discourses the literature review in more details which includes the effects of nanoparticles on ZnO based device. It also covers the ZnO based ultraviolet detection

Chapter 3

This chapter includes the synthesis and properties of material, in which we cover all the important properties of ZnO materials

Chapter 4

This chapter discusses about simulator methodology i.e. Optoelectronics simulator we used for the simulation of ZnO based UV photo transistor (PD) in more detailed way.

Chapter 5

This chapter includes the result discussion part, in which we obtained all the result by using ATLAS^{TM} simulator of SILVACO international.

Chapter 6

It includes the summary and conclusion of the dissertation. Important results of present study are summarized in the chapter. A brief discussion of future scope in related areas is covered in this dissertation.

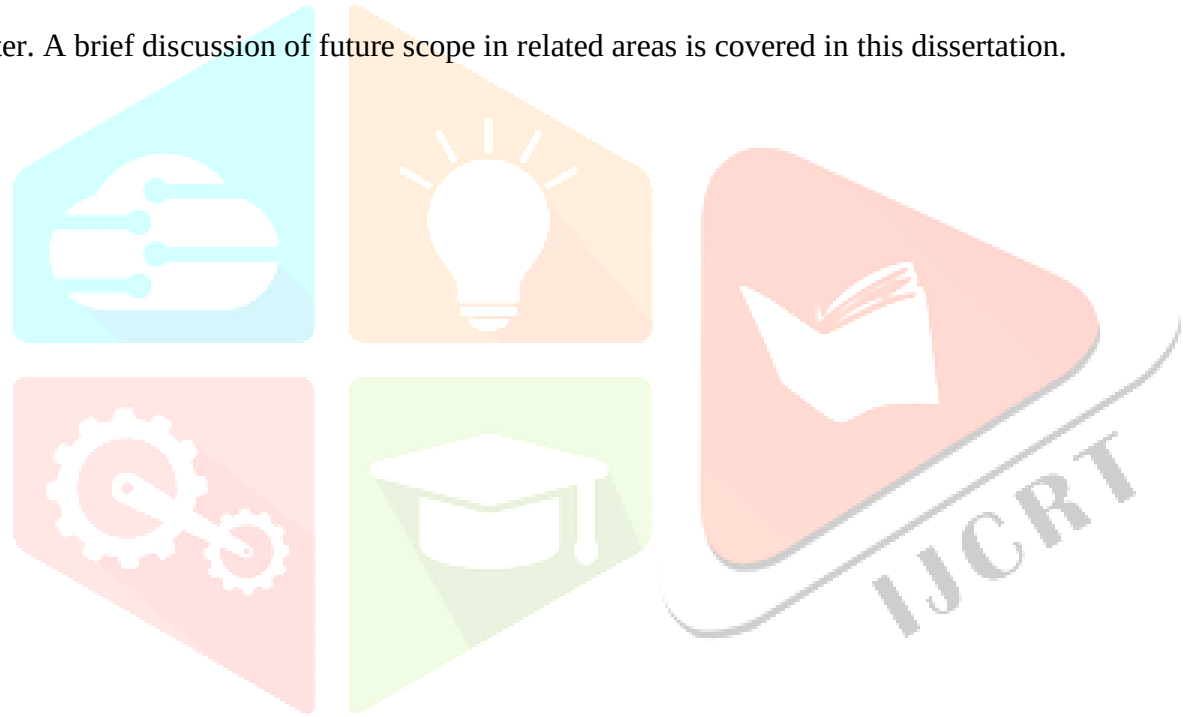

CHAPTER 2

2 REVIEW OF LITERATURE

In 1930s, when the invention of the Thin Film Transistor was patented, the basic principle is known today as the metal-semiconductor field-effect transistor (MESFET). Later on, insulating materials (such as aluminum oxide) was introduced between the semiconductor (copper sulfide) and the field-effect electrode (aluminum), forming the so-called metal-insulator-semiconductor field-effect transistor (MISFET) [13]. In 1962, RCA laboratories reported the fabrication of a TFT using thin films of polycrystalline Cadmium Sulfide (CdS) as the semiconductor material. Since the mid-1980s, silicon-based TFTs have become the most important devices for active-matrix liquid crystal displays (AMLCDs). In the past ten years, amorphous silicon (a-Si:H) TFTs have successfully dominated the large-area LCD product market. Meanwhile, research and development activities on polycrystalline silicon (poly-Si) TFTs are steadily increasing [14, 15]. More recently, a new generation of oxide semiconductors are being studied and applied as the active material to the TFT device, particularly the zinc oxide (ZnO) and In GaZnO (IGZO) thin films.

Currently, transparent electronics are one of the most advanced topics for a wide range of device applications, including invisible electronic circuitry, next generation displays, and optoelectronic devices. The key components of the transparent electronics are transparent conductive oxides (TCOs). TCOs are a special class of materials which possesses both high visual transparency due to their large band gap energy and high electrical conductivity. One of the most commonly used TCOs is ZnO, and the birth of transparent electronics is normally associated with the reports on ZnO TFTs presented in 2001-2003 [16, 17].

Because the ZnO is transparent in the visible region of the spectra, it is less light sensitive. Besides, the primary advantage of transistors using ZnO as active channel layer is the high electron channel mobility and the corresponding higher drive current and faster operating speeds. Another predominant advantage is that ZnO can be

deposited at or near room temperature with high-quality polycrystalline structure, which is compatible with the use of flexible substrate under lower processing temperature. In GaZnO (IGZO) is currently emerging as the preferred semiconductor for high performance and transparent large-area electronics. The advantage of IGZO material is its amorphous state compared to polycrystalline ZnO. The disorder in the IGZO system is comparable to a-Si:H thin films, providing excellent electrical uniformity over large areas compared to polycrystalline materials while possessing higher field-effect mobility's compared to a-Si:H.

ZnO being a high bandgap material is found to be transparent, letting all the wavelengths of the visible spectrum to pass through it. Due to these properties it finds application in displays, replacing poly-Si and a-Si:H devices. The fabrication process of this material is also straight forward and cost effective. Mostly RF magnetron sputtering technique is employed in its fabrication [18].

ZnO can be converted into insulator, semi-conductor and a metal just by controlling the doping level, keeping the transparent property all the while hence best suited in flat panel displays and solar cell applications. Naturally ZnO is N-type conductivity configuration but if P-type like conductivity were achieved with repeatability, then ZnO would establish itself as the most preferred material in opto-electronic industry. ZnO is one of the most promising materials among various semiconducting metal-oxides, because of its range of electronic, optical, magnetic and chemical properties. ZnO is most widely used oxide semiconductor with applications ranging from medical, agriculture, ceramic, and chemical to electronics and photonics [19, 20]. ZnO has been recognized in recent times as one of the most potential candidates for the next generation of transparent and flexible electronics for display systems in the form of transparent thin film transistors (TTFTs) [21-22]. The current technology based on amorphous or polycrystalline Si and organic semiconductors has severe electronic limitations due to low mobility ($\leq$ 1cm2/V s) and inadequate light sensitivity.

Currently it has been suggested that Wurtzite structured ZnO thin films could be used as the active channel layer in Transistors because of its low cost, easy availability, high mobility and no environmental concerns. Furthermore,

unlike Si Transistors and poly-Si Transistors, ZnO based Transistors are transparent in the visible region of the spectra and less visible light sensitive because of the large bandgap (3.4eV) of ZnO [23]. Another possible application involves use of ZnO TTFTs as transparent select-transistors in each pixel of an active-matrix liquid-crystal display (AMLCD) [24].

The important figures of merit that determine the performance of Thin Film Transistors are the magnitude of the field effect mobility, threshold voltage, and the drain current on/off ratio. A high value of channel mobility ensures a higher drive current density and a faster switching speed of a Thin Film Transistors. Considerable effort has been made to achieve high field-effect mobility and to understand the mechanism of operation of Thin Film Transistors in order to realize the key factors behind high performance and stability of these devices. In the recent past the field-effect mobility was reported to be ~25 cm2/Vs in a polycrystalline channel layer [25, 26] and as high as ~70cm^2/V-s in a single-crystalline channel layer [27].

Ever increasing interest in the ZnO based transistors has motivated the researchers to explore various techniques for growing ZnO films. These include RF-sputtering [28, 29] pulsed laser deposition (PLD) [30], spray pyrolysis [31], atomic layer deposition (ALD) [32], sol-gel [33, 34], thermal oxidation of Zn thin films [35] and chemical bath deposition [36]. Among these techniques sol-gel method has certain advantages, such as good reproducibility, simplicity, low cost, and high throughput that enable the fabrication of high-performance and low-cost electronics. In addition to these merits, it may also be possible to use sol-gel technique to realize high electron mobility.

Information on how ZnO films (grown by different methods) influence the mobility and hence the performance of Transistors is not available in the literature. In this paper, we investigated the characteristics of a suitable ZnO thin film for an active channel layer of ZnO based transistors. It was found that different deposition techniques of ZnO layer produce different electrical properties for the final devices. Theoretical study of these above mentioned Transistors is also carried out by ATLAS simulator; these theoretical results were further compared with experimental results.

ZnO is also known to have a capacity to detect ultraviolet photons (UV) [37]. Park et al. [38] and Jeong et al. already reported on the fabrication and electrical properties of n-ZnO/p-Si photodiodes that are able to detect visible and UV photons, respectively. Therefore, it is quite natural to see if ZnO-based Transistors have capabilities to detect UV and possibly visible photons. In the present paper, we report on the simulation of ZnO-based Transistors on p-Si substrates and particularly focus on their photo-detection capabilities.

Ultraviolet (UV) photodetectors have been widely used in various commercial and military applications, such as secure space-to-space communications, pollution monitoring, water sterilization, flame sensing and early missile plume detection, etc. [39]. All these applications require very sensitive devices with high signal-to-noise ratio and high response speed.

A variety of UV detectors are available, mainly Si-based photodetectors and photomultipliers. These devices can be very sensitive in UV region with low noise and quick response. However, they have significant limitations, such as the need of filters to stop low energy photons (visible and IR light), their degradation and lower efficiency (Si-based photodetectors), or the need of an ultra-high vacuum environment and a very high voltage supply (photomultipliers) [40]. To avoid these disadvantages, UV detectors based on wide bandgap semiconductors (such as diamond, SiC, III-nitrides and wide-bandgap II–VI materials) have received more and more attention due to their intrinsic visible-blindness. Moreover, wide-bandgap materials are chemically and thermally more stable, which is an advantage for devices operating in harsh environments [41].

Among them, ZnO has been studied extensively in recent years for their unique properties and potential applications of electronic and optoelectronic devices [42, 43]. It has strong radiation hardness, high chemical stability, low cost, and a large bandgap of 3.37 eV at room temperature. Furthermore, doping in ZnO with Mg elements can adjust the bandgap and make it feasible to prepare UV photodetectors with different cut-off wavelengths [44, 45].

The UV photo response in ZnO films was first observed by Mollow in the 1940s [46]. However, the research of ZnO based photodetectors flourished gradually since the 1980s [47]. At the beginning, the devices usually have simple structure and the properties are not very good. With improvement of the fabrication of the ZnO-based films using different techniques, many complex ZnO-based photodetectors (such as p-n junction, p-i-n junction and Schottky junction, etc.) with high performance were reported. In this paper, we review the recent progress in ZnO-based photodetectors.

Over the past decade, zinc oxide (ZnO) has attracted increasing interest for its particular properties, such as a wide band gap of~3.37 eV, high radiation endurability, low visible absorption, low cost, and it is environmentally friendly as well, which makes ZnO a promising material for ultraviolet (UV) photodetector applications[48－49] ZnO-based UV photodetectors have been fabricated from single crystals, thin films and nanostructures in recent years[50－55] Increasing the performance is still one of the major issues of ZnO-based UV photodetectors, and continuing efforts have been devoted to this issue[56－62] Recently, much attention has been paid to surface plasmons (SPs) for their fundamental scientific importance and promising practical applications.[62－68]

The SPs can be realized in coatings on the surface of metal nanoparticles (NPs) by magnetron sputtering. [69] The metal NPs on the surface can enhance the scattering of the incident photons and make more photons reach the substrate, and thus the absorption of the photons can be enhanced [70－71] which provides a novel idea of enhancing the performance of ZnO UV photodetector.

In this paper, we report the growth of ZnO thin films on quartz substrates by a radio frequency (RF) magnetron sputtering technique, and focus on Metal NPs enhancement on the performance of ZnO-based metal－

semiconductor−metal (MSM) Schottky UV photodetectors, and then verify the enhanced by FDTD method. Pt NPs on the surface of photodetector make the responsivity significantly enhanced, which demonstrates that this method is a promising route to improve the performance of ZnO based photodetectors.

Chapter 3

3 Synthesis and Properties of Materials

1 Zinc oxide (ZnO)

Zinc oxide is an inorganic compound with the formula ZnO. It usually appears as a white powder, nearly insoluble in water. The powder is widely used as an additive into numerous materials and products including plastics, ceramics, glass, cement, rubber (e.g. car tyres), lubricants, paints, ointments, adhesives, sealants, pigments, foods (source of Zn nutrient), batteries, ferrites, fire retardants, etc. ZnO is present in the earth crust as a mineral zincite; however, most ZnO used commercially is produced synthetically.

In material science, ZnO is often called an II-VI semiconductor because zinc and oxygen belong to the 2nd and 6th groups of the periodic table, respectively. This semiconductor has several favorable properties: good transparency, high electron mobility, wide band gap, strong room temperature luminescence, etc. Those properties are already used in emerging applications for transparent electrodes in liquid crystal displays and in energy-saving or heat-protecting windows and electronic applications of ZnO as thin-film transistor and light - emitting diodes.

Zinc oxide (ZnO) is a unique material with a direct band gap (3.37eV) and large exciton binding energy of 60 meV, which makes the exciton state stable even at room temperature. ZnO has been widely used in near-UV emission, gas sensors, transparent conductor, thin film transistors and piezoelectric applications.

Zinc is also a very important trace element in humans. The average adult body contains 2-3 gram of zinc, which is found in muscle, bone, skin and plasma. Significant amounts occur in the liver, kidney, eyes, hair etc. Zinc has been found to play an important part in many biological systems. Therefore, ZnO is environmentally friendly and suitable for in- vivo bio-imaging and cancer detection

2 Fundamental properties of ZnO

.1 Crystal structure

Zinc oxide crystallizes in three forms: hexagonal wurtzite, cubic zinc blend, and the rarely observed cubic rock salt. The wurtzite structure shown in fig 3.1 is most stable and most common at ambient conditions. The zinc blend form can be stabilized by growing ZnO on substrates with cubic lattice structure. In both cases, the zinc and oxide are tetrahedral. The hexagonal and cubic zinc blend ZnO lattices have no inversion symmetry (reflection of a crystal relatively any given point does not transform it into itself). This and other lattice symmetry properties result in piezoelectricity of the hexagonal and zinc blend ZnO, and in pyro electricity of hexagonal ZnO.

The lattice constants are a = 3.25 Å and c = 5.2 Å; their ratio c/a ~ 1.60 is close to the ideal value for hexagonal cell with c/a = 1.633. As in most II-VI materials, the bonding in ZnO is largely ionic, which explains its strong piezoelectricity. Due to this ionicity, zinc and oxygen planes bear electric charge (positive and negative, respectively).

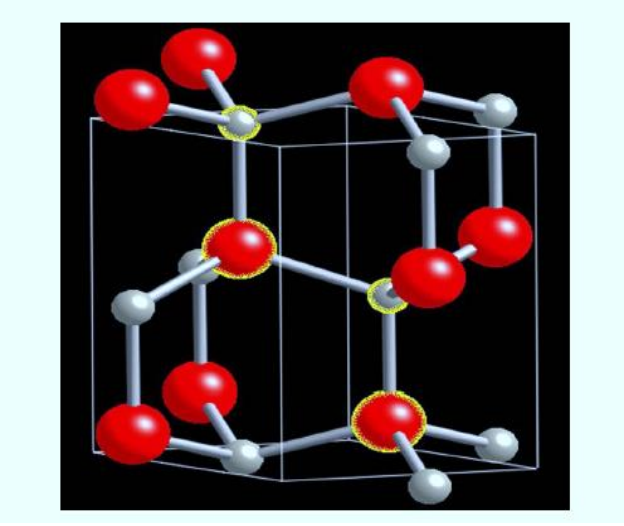

Figure 3-1 Schematic representation of a wurtzitic ZnO structure

.2 Physical properties of ZnO

I have mentioned the Physical properties of ZnO in Table 3.1 Still some uncertainty exists in these values. For example, in few reports it has been mentioned physical properties of only p-type ZnO and therefore the hole mobility and effective mass are still in debates.

Table 3-1 Basic physical properties of ZnO

Property	value
Lattice parameter at 300K	
A	3.2495
C	5.2069
c/a	1.602
Density	5.606g/cm^3
Stable phase at 300K	Wurtzite
Bond Length	1.977μm
Melting Point	1975°C
Thermal conductivity	0.6,1-1.2
Static dielectric constant	8.656
Refractive index	2.008,2.029
Energy gap 3.4 ev,	Direct
Excition binding energy	60mv
Iconicity	62%
Heat capacity	9.6cal/mol K
Young's modulus E	111.2±4.7Gpa

.3 Optical properties of ZnO

The study of optical properties particularly for ZnO has been carried out over the past few decades. To date ZnO has drawn Mach attention based on its unique and promising properties that makes it a promising candidate for short wavelength photonics. These properties arise from its direct wide band gap of 3.37 eV which corresponds to the energy of 3655A° photons.

ZnO is a material that strongly absorbs ultra violet light below 3655A° and is transparent to visible wavelength of the electromagnetic spectrum. Zinc oxide generally appears as white in the range of visible wavelengths with a typical refractive index of 2.008. But due to unintentional doping of the grown crystals ZnO crystals usually appears as red, green or yellow colored. Under ultra violet (UV) light ZnO becomes photo-conductive. By the combination of optical and semiconductor properties, doped zinc oxide becomes a contender for a new generation of devices.

.4 Electrical properties of ZnO

As a direct and wide band gap semiconductor with a large exciton binding energy (60meV), ZnO is representing a lot of attraction for optoelectronic and electronic devices. For example, a device made by material with a larger band gap may have a high breakdown voltage, lower noise generation and can operate at higher temperatures with high power operation. The performance of electron transport in semiconductor is different at low and high electric field. At sufficient low electric fields, the energy distribution of electrons in ZnO is unaffected much, because the electrons can't get much energy from the applied electrical field, as compared with their thermal energy. So the electron mobility will be constant because the scattering rate, which determines the electron mobility, doesn't change much.

When the electrical field is increased, the energy of the electrons from the applied electrical field is equivalent to the thermal energy of the electron. The electron distribution function changes significantly from its equilibrium value. These electrons become hot electrons, whose temperature is higher than the lattice temperature. So there is no energy loss to the lattice during a short and critical time. When the electron drift velocity is higher than its steady state value, it is possible to make a higher frequency device.

.5 Chemical Properties

ZnO occurs as white powder commonly known as zinc white or as the mineral zincite. The mineral usually contains a certain amount of manganese and other elements and is of yellow to red color. Crystalline zinc oxide is thermo-chromic, changing from white to yellow when heated and in air reverting to white on cooling. It is nearly insoluble in water and alcohol, but it is soluble in (degraded by) most acids, such as hydrochloric acid:

$$ZnO + 2\ HCl \rightarrow ZnCl_2 + H_2O$$

Bases also degrade the solid to give soluble zincates:

$$ZnO + 2NaOH + H_2O \rightarrow Na_2\ (Zn\ (OH)_4)$$

ZnO reacts slowly with fatty acids in oils to produce the corresponding carboxylates, such as oleate or stearate. ZnO forms cement-like products when mixed with a strong aqueous solution of zinc chloride and these are best described as zinc hydroxyl chlorides. This cement was used in industry. ZnO also forms cement-like products when reacted with phosphoric acid, and this forms the basis of zinc phosphate cements used in dentistry.

.6 Thermal Properties

3.2.6.1. Thermal expansion coefficient (TEC)

The change in temperature affects the lattice parameters of semiconductors. Thermal expansion coefficients are defined as α_a and α_c for in and out of plane cases, respectively. The stoichiometry, presence of extended defects and free carrier concentration also affect the thermal expansion coefficient. The X-ray powder diffraction method by Reeber was used to measure the temperature dependence of lattice parameters of ZnO as shown in (Figure 3-2).

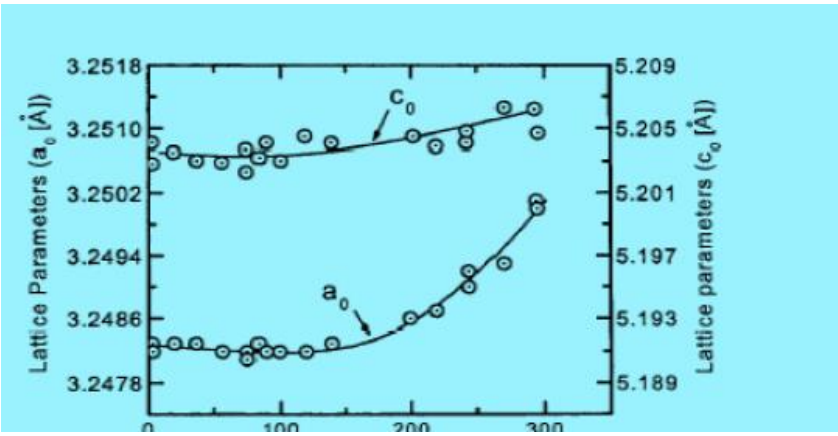

Figure 3-2 Wurtzite ZnO lattice parameters as a function of temperature

6.2 Thermal conductivity

It is really important property of semiconductors when these materials are used in high-power, high-temperature or optoelectronic devices. The electronic thermal conductivity is very small, having light carrier concentration, which is negligible. Fig.3.3 shows the thermal conductivity curve for a fully sintered ZnO crystal. The thermal conductivity decreases from 37 to 4 W/m K as the temperature is increased from room temperature to 1000°C

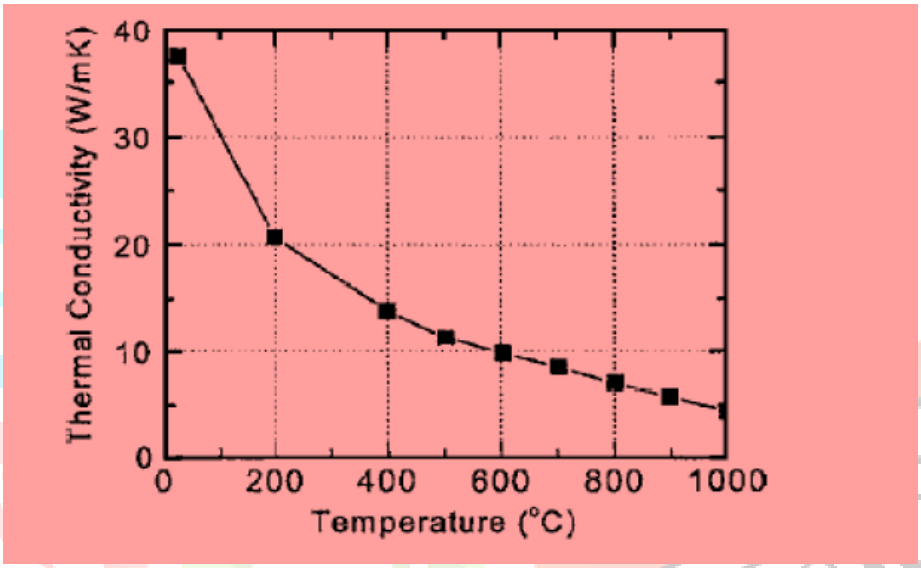

Figure 3-3 Thermal conductivity of fully sintered ZnO heated from room temperature to 1000°C

Chapter 4

4 SIMULATION TOOL AND ITS METHOD

4.1 Introduction

Atlas is a software provide general potentials for physical-based two and three dimensional

(2D, 3D) simulation of semiconductor devices. Atlas is designed in such a way that it can be used with the VWF interactive tools. The VWF (Virtual wafer fabrication) interactive tools consist of the following: MaskViews, Optimizer, Deck Build, TonyPlot, and DevEdit. Their Functions are explained below [73-75].

- DeckBuild puts forward the condition for running Atlas command language.
- crafting a device structure and specifying the meshes used in it require a cooperative

  Surrounding which is made available by DevEdit.
- Optimization across various simulators can be provided by optimizer.
- IC layout correction is done by MaskViews.
- Through TonyPlot the outputs which are actually the electrical characteristics of the device and the structure files generated for the designed device can be seen.

Through these VWF Tools simulation results can be closely related to advancement of technology and also reflects that the research of the devices was done experimentally. Hence for the approaching semiconduor technology, these tools can prove to be very beneficial. it is also the approaching semiconductor technology,these tools can prove to be very beneficial.it is also very useful for prediction of all the characteristics and features of the new devices and processes of technology.

Along with Atlas, there exists another process simulator, Athena. It can produce structures

Prepared by many processing steps. The same structures can be utilized by Atlas as inputs. Later Atlas predicts the different electrical characteristics related to the designed device. Now the outputs of the Atlas can be given as the used as the inputs to the SPICES modeling Software and Utmost devices characterization.

Atlas can also be called as a physically-based simulator for devices as it is capable of calculating all the characteristics associated with a particular devices with specified structure and voltage at the electrodes. The whole devices area is divided by these simulators with grids Voltage biases at the electrodes. The whole devices area is divided by these simulators with grids called “meshes” and with mesh points called “nodes”. By applying differential equations which are derived from Maxwell’s Laws, current conduction and electrical parameters at each location through the structure is determined. This type of physically based simulation has many advantages like ,they provide a deep insight of the attributes of a device without experimentally creating the device, calculation of very complex parameters are done very easily and quickly, estimation of the trends with the varying properties of the devices according to its different bias conditions can be estimated through these simulations.

2 ATLAS Input and Output

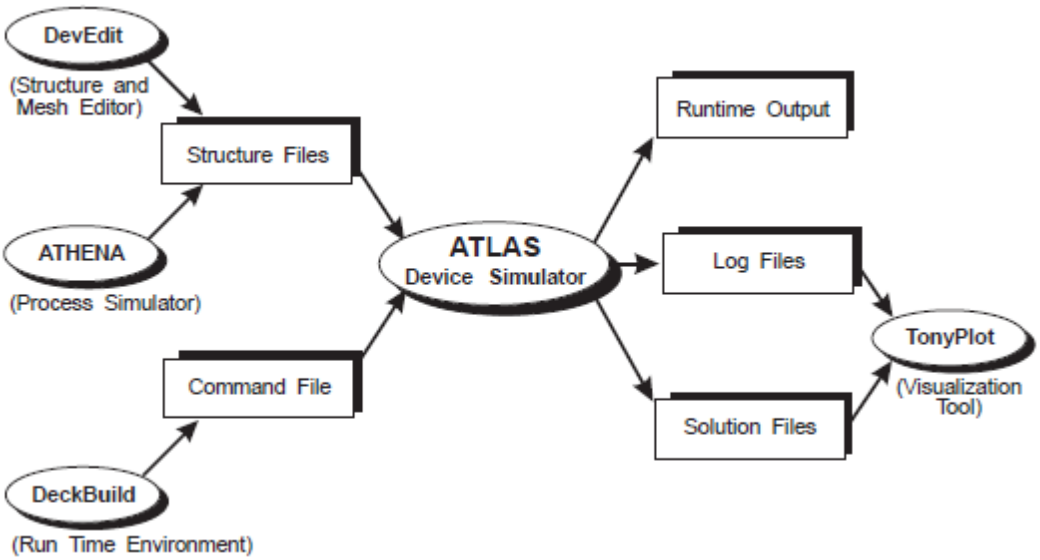

Figure 4-1 Inputs and Outputs Flow of ATLAS device simulator.

Information’s flowing through Atlas device simulator can be seen in the above diagram (Figure4.1). The text file, which contains Atlas command language and structure file, which has the structure on which simulations has to be

performed are the two input files to Atlas device simulator. Atlas has three types of output files: runtime output which gives the information being processed at every instant of execution of atlas command and simultaneously show the errors and warnings, log files which gives all the electrical characteristics which is specified in the Atlas command language and solution files which has the 2D or 3D data of the device parameters at each and every point in the device[73]

4.3 Using ATLAS Commands to define a structure.

At first we need to define mesh while defining a structure in ATLAS. This mesh can be explained as a sequence of horizontal and vertical streaks and spaces between these lines. Regions inside this mesh are assigned to dissimilar materials according in the direction of our requirement intended for constructing proposed device. After defining regions next step is to specify the electrode and at last the doping of each region is need to be specify.

4.3.1 Initially we need to define the Mesh which can be written using the command language as:

Table 4-1 Syntax for Initial Mesh Specification.

Statement	Comment
Mesh space.mult=<value>	Spac.mult factor cast-off as a factor aimed at the obtained mesh by the declarations x.mesh and y.mesh. This will be one for default case and lesser value will create finer mesh.
x.mesh location=<value> spacing=<value> y.mesh location=<value> spacing=<value>	These two statements used to state the positions in microns of vertical and horizontal streaks along by way of spacing associated to each line. It should be state with the increase order of x and negative value also allowed

2 Region and Material Specification

After defining the mesh next step is to define each part with a material type which is done through REGION statements as follows:

Table 4-2 Syntax for Specifying Region and Material.

REGION num=<integer> / <material type> <position parameters>	Region number should begin with one and increases for each succeeding region. The position constraints are defined by using x.minimum,x.maximum,y.minium,y.maxmium in microns.

3 Electrode Specification

Once specifying the region and material we need to define electrode that works as a contact for the semiconductor using the command as follows:

Table 4-3 Syntax for Specifying Electrode.

Statement	Comment
ELECTRODE NAME=<electrode name><position parameter>	The position parameters are described by using x.max, x.min, y.max, y.min in microns.Upto 50 electrodes can be specified with same name also.

4 Doping Specification

Doping profile can vary with its concentration and type of doping which are specified by value and doping type respectively. The doping profile can be either is uniform or Gaussian. To introduce the contacts the following syntax is required:

Table 4-4 Syntax for Doping Specification.

DOPING <distribution type><dopant type><position parameters>	Doping profile can either be Gaussian or uniform.

For example:

DOPING CONCENTRATION=1E18 P.TYPE GAUSSIAN CHARACTERISTIC=0.5 X.LEFT=1.0 X.RIGHT=2.0 PEAK=0.1

This declaration specifies a p-kind of Gaussian profile by means of a peak concentration of 1018/cm3 topmost doping positioned sideways a line on or after x=1 to x= 2 microns.

4.4 Specification of models

Usually the statements for MODELS are used to indicate the physical models which are required for simulations. The selection of the MODELS is according to the physical phenomenon occurring inside the considered device. These MODELS be divided into the following categories

4.4.1 Concentration-Dependent Low-Field Mobility Model:

To activate this model, CONMOB is used in the MODELS statement. This model provides the data for low field mobility's of electrons and holes at 300K for silicon and gallium arsenide only.

4.4.2 Shockley-Read-Hall Recombination Model:

The SRH parameter is used in the MODELS statement for activating this model. There are a few user-definable parameters that used in the MATERIAL statement, like TAUN0 and TAUP0the electron and hole lifetime parameters. This model indicates the recombination of electron and hole through Shockley-Read-Hall recombination method happening within the device.

3 Auger Recombination Model:

This model can be activated by specifying AUGER in the MODELS statement. The coefficients for electrons and holes for this model are user definable parameters. These coefficients, augn and augp, can be incorporated in the MATERIAL statement.

4 Boltzmann Model:

This model is the default carrier statistics model. It is activated by specifying BOLTZMANN in the MODELS statement. As the name indicates this model follows Boltzmann statistics.

5 Fermi-Dirac Model

This model follows Fermi-Dirac statistics. It is usually in those regions which are heavily doped but with reduced concentrations of carrier. To activate this model FERMI is used in the MODELS statement.

6 Numerical methods

The numerical methods are specified in the METHODS statement. To find solution there are three different types of techniques:

1. Gummel
2. Newton
3. Block

The first method finds solution for one unknown variable while the rest of the variables are

Constant. This process will continue until a stable solution is obtained. Unlike the gummel

Method, newton method solves and finds all the unknowns at the same time. Block method is in between newton and gummel methods as it solves a few unknowns at the same time gummel is generally used for the device like tunnel FET.

4.6 Methods to obtain solutions

To calculate current as well as other parameters such as carrier concentrations and electric fields, the device electrodes needs to be supplied with voltages. At first, electrodes are provided with zero voltages, after that the bias voltage applied is varied in small steps. These needs to be specified in the SOLVE statements.

4.6.1 DC Solution

A fixed DC bias can be applied on the electrode by using the DC solve statements.

SOLVE <v.electrode name>=<value>.

According to this statement the required electrode, electrode name is supplied with DC voltage value.

For sweeping the bias of a particular electrode from value1 to value2 in a particular order of steps step, the following command is used.

SOLVE <v.electrode name>=<value1> VSTEP=<step1> VFINAL=<step2>

NAME=<electrode name>.

Convergence can be obtained for the used equations by supplying a good original presumption for the variables that need to be evaluated at each bias point. Initial solution can be achieved by the given statement,

SOLVE INIT.

4.6.2 AC Solution

A simple extension of the DC solution syntax can specify the AC simulations. A post-processing operation to a DC solution leads AC small signal analysis. The conductance and capacitance between each pair of electrodes is the results of AC simulations. The command used for this is

SOLVE VBASE=0.7 AC FREQ=1e9 FSTEP=1e9 NFSTEPS=10

Optoelectronics device simulator (Luminous)

Luminous is a general purpose ray trace and light absorption program integrated into the ATLAS framework, which is used to run with device simulation products. Optoelectronic device simulation is split into two distinct models that are calculated simultaneously at each DC bias point or transient time step

1 Optical ray trace model

An optical beam is modeled as a collimated source using the BEAM statement. The origin of the beam is defined by parameters X.ORIGIN and Y.ORIGIN (see Figure 4.2). The ANGLE parameter specifies the direction of propagation of the beam relative to the x-axis. ANGLE=90 is vertical illumination from the top. MIN.WINDOW/MAX.WINDOW parameters specify the illumination window. As shown in Figure 4.2, the Illumination Window is "clipped" against the device domain so that none of the beam bypasses the device.

The beam is automatically split into a series of rays so that the sum of the rays covers the entire width of the illumination window. When the beam is split, ATLAS automatically resolves discontinuities along the region boundaries of the device.

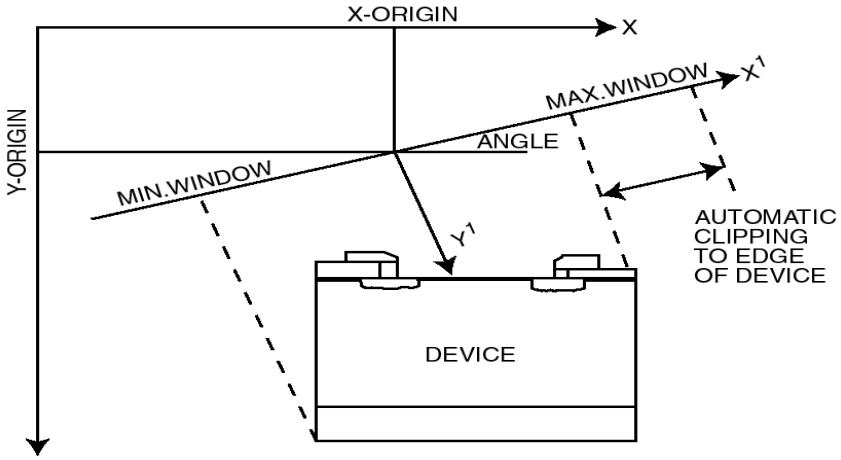

Figure 4-2 Optical Beam Geometry

Although the automatic algorithm is usually sufficient, you can also split the beam up into a number of rays using the RAYS parameter. Each ray will then have the same width at the beam origin and the sum of the rays will cover the

illumination window. Even when you specify the RAYS parameter, ATLAS will automatically split the rays to resolve the device geometry.

4.7.2 Generation of Photocurrent and Quantum Efficiency

One of the important figures of merit of a photodetector is quantum efficiency. Here, quantum efficiency is defined as the ratio of the number of carriers detected at a given photodetector electrode divided by the number of incident photons on the detector. LUMINOUS doesn't directly calculate quantum efficiency. It does, however, calculate two useful quantities printed to the run-time output and saved to the log file. These quantities are source photocurrent and available photocurrent, which can be viewed in TONYPLOT from log files produced by LUMINOUS.

The source photocurrent for a monochromatic source is given as:

$$I_s = q\frac{Bn\lambda}{\hbar c} W_t \quad \text{..... (12)}$$

- Here : Bn is the intensity of the beam number n

  λ is the source wavelength

  h is the Planck's constant which is equal to approximately 6.626176×10-34 J/s

  C is the speed of light which is equal to 2.99792458 x 108 m/s

  q Is the electronics charge which is equal to 1.6021765×10-19 coulomb

  W_t is the width of the beam

4.7.3 Photodetector simulation

This sections explains the technique is used for simulation of photodetectors which can be applied to avalanche photodiodes, CCDs, Schottky photodiodes, MSMs and other optical triggered devices

Defining Optical Sources

4.7.4.1. Recognizing an Optical Beam:

Photosensitive sources can be described by using BEAM statement which must be mentioned anywhere next to MESH, REGION, DOPING, and ELECTRODE statements and before SOLVE statement. Maximum ten optical sources can be defined. The NUM parameter used for unique identifying one photosensitive source whose value can

be varies from 1 to 10. B<n> parameter is used to set the power of the optical beam, everyplace n represents the beam digit demarcated by NUM.

4.7.4.2. Beam Origin Plane for Optical Sources:

Optical source origin can be used by using X.ORIGIN and Y.ORIGIN parameters which define the source of the optical beam qualified to the device coordinate structure. At present it should lie outside the device region. The direction of beam propagation with respect to the device coordinate system can be specified by using ANGLE parameter. ANGLE=90 shows vertical illumination from above. MAX.WINDOW and MIN.WINDOW parameter is used to specify the width of the optical beam.

.1 Obtaining Quantum Efficiency versus Bias

The intensities mentioned in the SOLVE declaration till another SOLVE statement modifies the intensity of the beam. Simple optical intensity of linear ramps can be specified using the NSTEP and LIT.STEP parameters in solve statement Where NSTEP describes the number of steps and LIT.STEP represents the size of the DC step.

.2 Finding Transient Reaction of Optical Bases

It is at times required to find out the time dominion output of the optoelectronic device to know the time dependent of the optical sources. RAMP.LIT parameter specified in LUMINOUS must be mentioned in a SOLVE declaration where the optical power will change from the utmost lately set strength to the given power mentioned in B parameter.

The RAMPTIME parameter will specify the linear ramp period and TSTOP parameter specifies where the transient simulation will stop. TSTEP also should be set for transient response which allows several samples within the RAMPTIME. Sample example shown below gives the specification for an optical source [15].

For example:

SOLVE B1 RAMPTIME=10E-9 TSTOP=30E-9 TSTEP=1E-11

7.3.3 Obtaining the Spectral Response

The device current as a function of wavelength called as spectral response can be found. The LAMBDA factor in SOLVE statement use to fix the wavelength of the beam in microns. We should specify the initial and final wavelength and the step size of the wavelength as mentioned below:

SOLVE BEAM=1 LAMBDA=0.2 WSTEP=0.1 WFINAL=0.8

Here the spectral response is obtained for initial wave length given 0.2 microns till 0.8 microns (WFINAL) with a step size of 0.1 microns.

7.3.4 Obtaining Angular Response

The output of detector also can be found out with respect to angle of incidence by using the following:

SOLVE BEAM=1 ANGLE=0.0 ASTEP=10.0 AFIANL=60.0

This allows collection of response versus angle. Here we get angular response from 0 degree to 60 degree with a step of 10 degree.

4.8 Prediction of results

The output files of Atlas are of three different types. They are:

4.8.1 Run-Time Output

The output seen at the bottom of the Deck Build Window is the run-time output. Any errors occurring during this output will be displayed in the run-time window.

4.8.2 Log Files

These files are required for storing the terminal characteristics calculated by Atlas. It consists of the current and voltages for each electrode during the DC simulations. In transient simulations, the time is saved. Whereas for AC simulations, the conductance, capacitances and the small signal frequency are stored.

4.8.3 Extraction of parameters In Deck Build

For this the EXTRACT command is introduced inside the Deck Build environment. Thus extracting the various parameters of the device. The command has a flexible syntax that allows you to construct specific EXTRACT routines. EXTRACT can operate on the earlier solved curve or structure file.

CHAPTER 5

5 SIMULATION RESULTS & DISCUSSION

.1 Introduction

In this chapter, all the simulation results and its discussion are briefly described for the ZnO based Ultraviolet Photo-Transistor. In this chapter, firstly we have drawn drain characteristics, transfer characteristics, transient response, spectral response and responsivity with and without plasmonic by using SILVACO software. We found that the result obtained from simulation is approximately equal to practical result. It was observed that there is an appreciable increase (factor of 100) in drain current, photocurrent and all the other parameter with a plasmonic layer.

Simulation studies were done on:

(a)Simple device structure of ZnO based Photo-Transistor

(b)ZnO based Photo-Transistor without plasmonics

(c)ZnO based Photo-transistor with plasmonics

.2 DEVICE STRUCTURE AND SIMULATION MODELS:

The device structure is shown in figure 5.1 in which we define the following region:

Reg.1: drain region of length $1\mu m$ and width $0.02\mu m$

Reg.2: source region of length $1\mu m$ and width $0.02\mu m$

Reg.3: ZnO layer of length $12\mu m$ and width $0.05\mu m$

Reg.4: silicon substrate of length $1\mu m$ and width $0.02\mu m$

Reg.5: gate region of length $12\mu m$ and width $0.04\mu m$

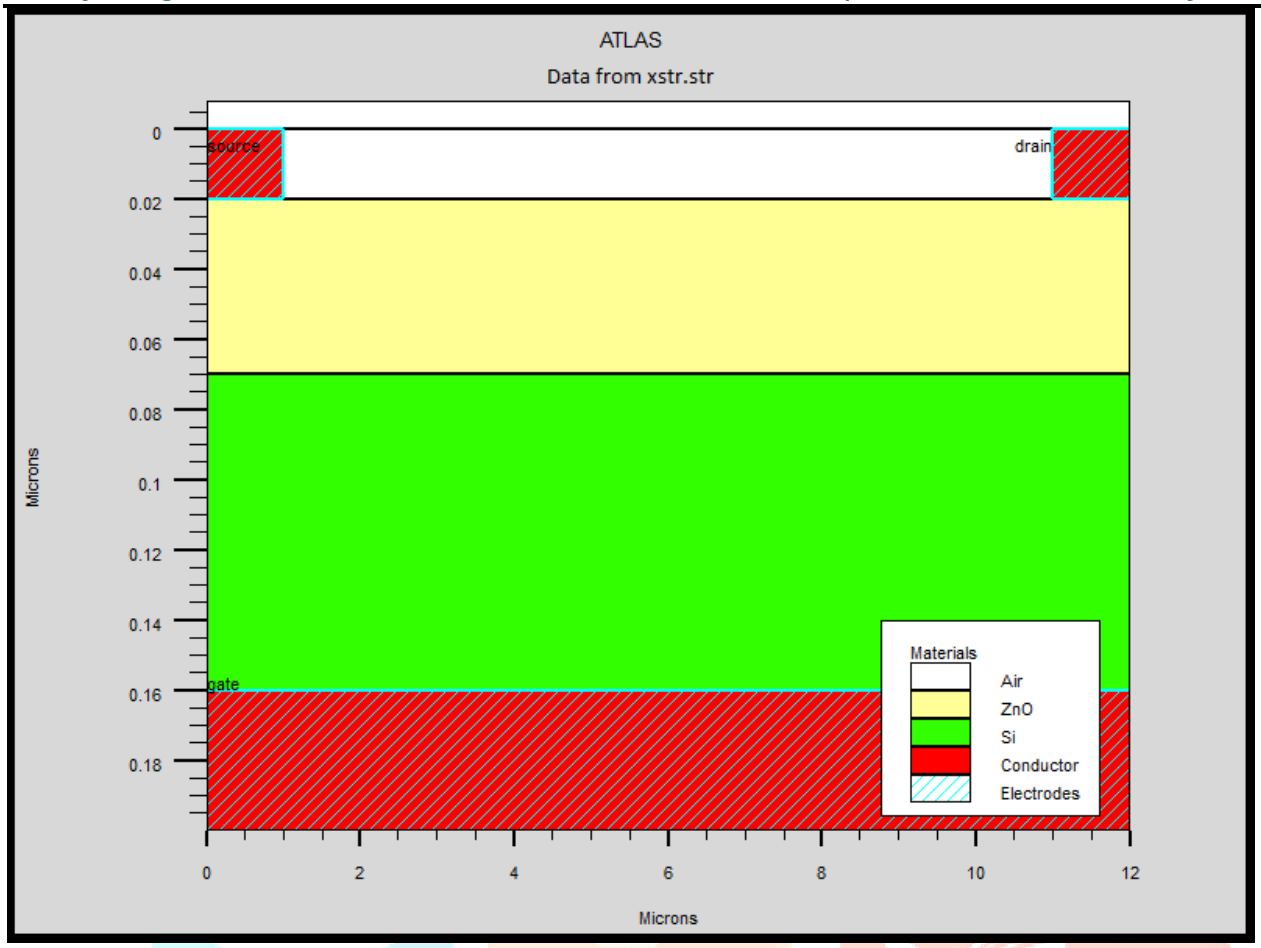

Figure 5-1 Simulated Structure of ZnO based Photo-Transistor

Table 5.1 contains the various parameters, which are used in the simulation of the device structure. In the given figure we use Titanium for making the electrode like source, drain and gate, all the electrode are doped uniformly. The electrode is made contact with ZnO, Which perform N-Type behavior of semiconductor. Zinc oxide (ZnO) is a unique material with a direct band gap (3.37eV) and large exciton binding energy of 60meV, which makes the exciton state stable even at room temperature. In the given figure 5.1 we use the doping concentration of ZnO is 1×10^{17} /cm^3. Further we use a P-type silicon substrate with doping concentration of 1×10^{15}/cm^3.

Table 5-1 Specifications of device parameters

Parameters	Symbol	Values	Unit
Source work- function	ϕ_M	5.1	eV
Drain work-function	ϕ_M	5.1	eV
Gate work-function	ϕ_M	4.6	eV
Channel Doping	N_D	10^{17}	cm^{-3}
Substrate Doping	N_{SUB}	10^{15}	cm^{-3}
Channel Length	L	10	μm
Gate voltage	V_{GS}	-0.5 to-1.0	V
Drain voltage	V_{DS}	0 to 2.5	V
Substrate voltage	V_{SUB}	0	V

.3 Drain characteristics

Drain characteristics is drawn between drain current and drain voltage. The figure 5.2(a) shows the graph between drain current and drain voltage, in which current is saturated to 3.1×10^{-7}A when we supply drain voltage more than 0.4V.

Now we check the effect of light on the same device under same condition, for this purpose, we incident a beam of light vertical (90°) at the midpoint (6, 0.02) on the device. Beam of light contains a wavelength of 350nm and beam intensity of 550mw/cm^2 . After falling the light we found that the current increase approximately 10 times more than the current which are obtained when we not incident light on the device, in this case the drain current saturated to 2×10^{-6}A after supply voltage more than 0.7V which are shown in figure 5.2(b). Hence this device is capable for detection of ultra-violet (UV) light. From the above conclusion we observed that this device full-fill our desired response .Due to direct band-gap (3.37eV) and large excitation binding energy (60mev) ZnO play an important role for detection of light.

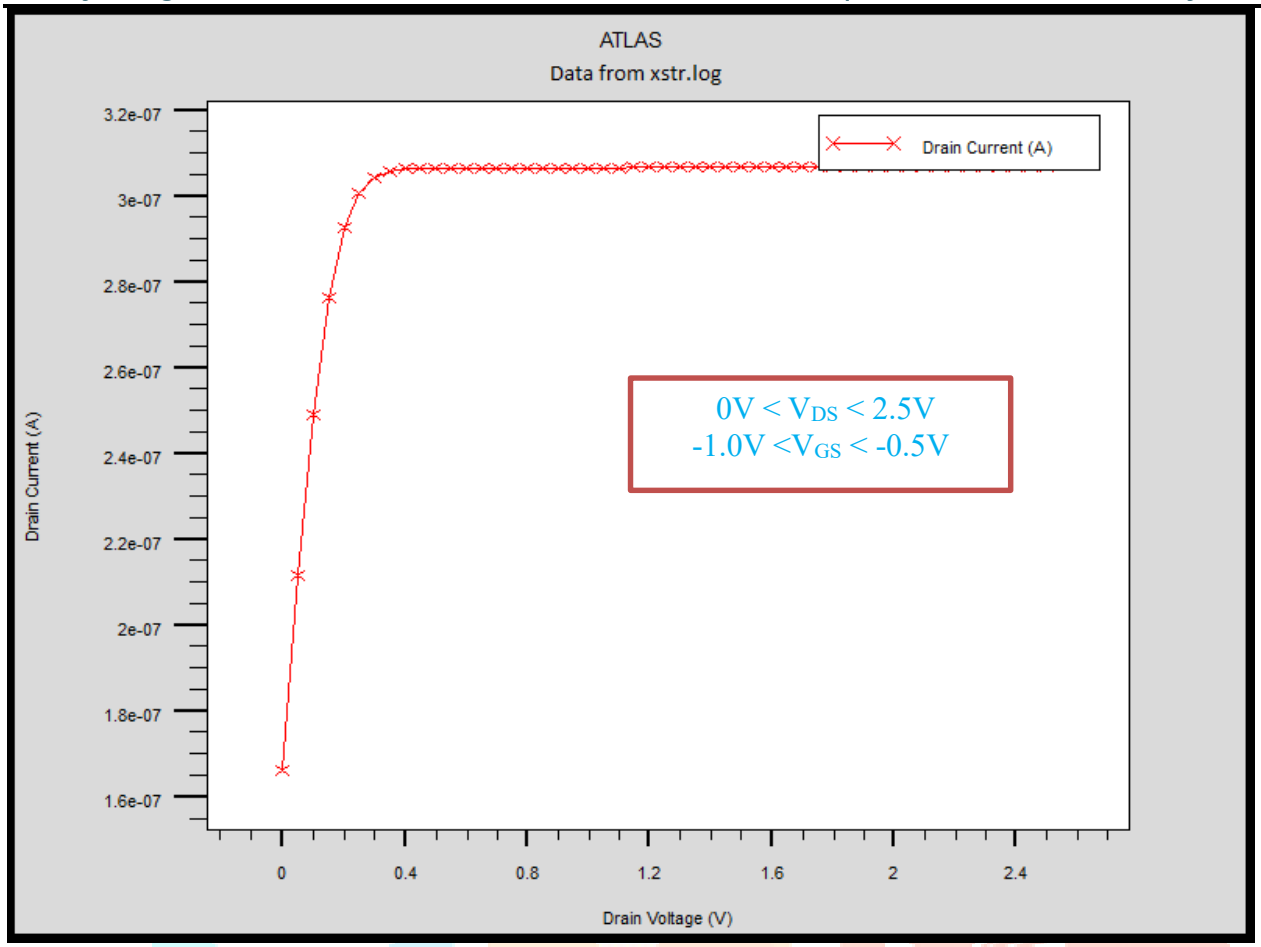

Figure 5-2(a) Drain current (I_D) versus Drain voltage (V_D) without light

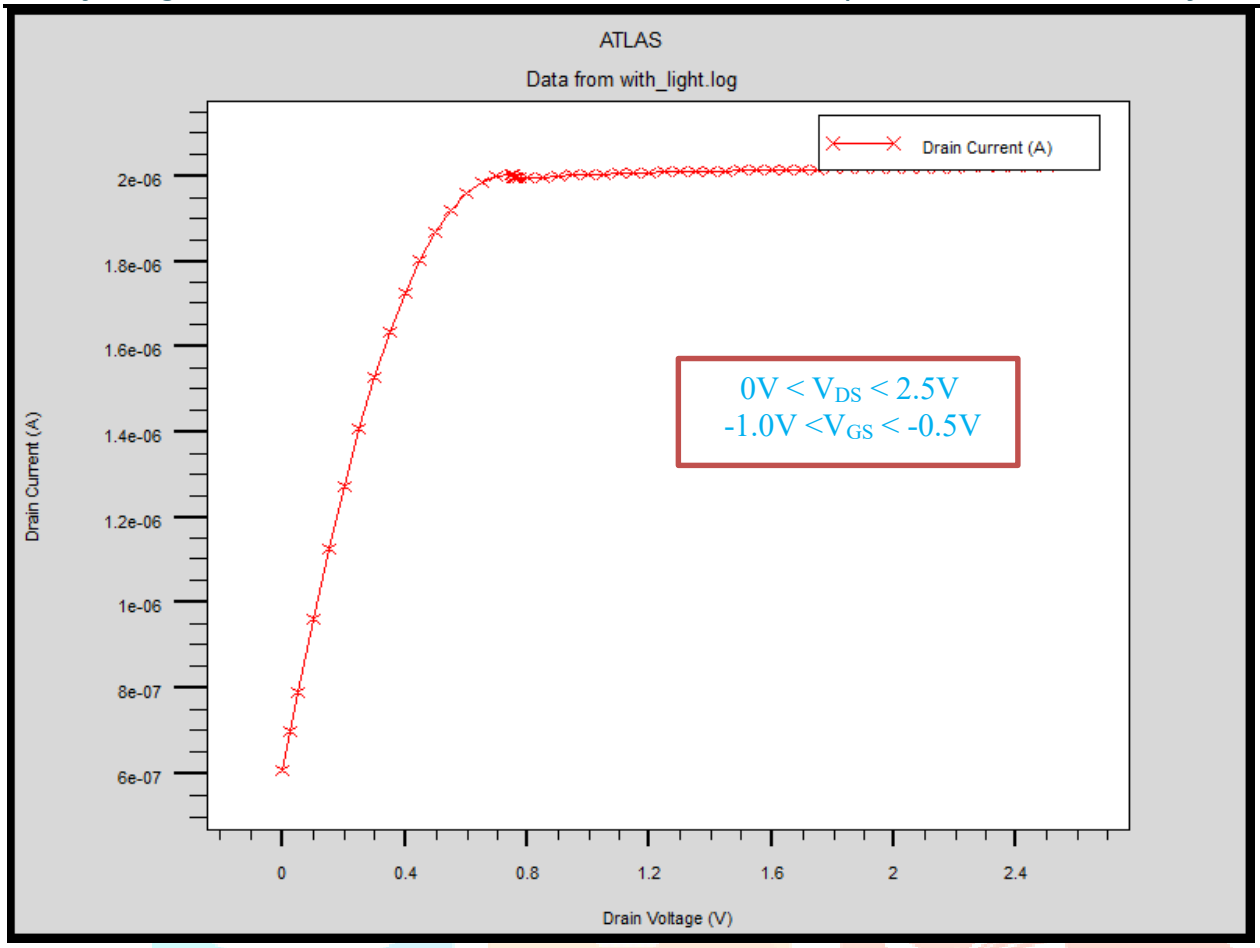

Figure 5-2(b) Drain current (I_D) versus Drain voltage (V_D) with light

.4 Transfer characteristics:

Transfer characteristics draw the plot between drain current (I_D) versus gate voltage (V_G).The figure 5.3(a) shown the graph between drain current versus gate voltage, in which drain current increase with increase in input voltage .The maximum drain current(I_D) is 3.29×10^{-7}A at -0.5 gate voltage(V_G).

Now we check the effect of light on the same device under same condition, for this purpose, we incident a beam of light vertical (90°) at the midpoint (6, 0.02) on the device. Beam of light contains a wavelength of 350nm and beam intensity of 550mw/cm^2. After falling the light we found that the current increase approximately 10 times more than the current which are obtained when we not incident light on the device, in this case the drain current increased linearly with increase in gate voltage and attained a maximum value (2.1×10^{-6}A) at gate voltage -0.5V which are shown in figure 5.3(b). From the above conclusion we observed that this device full-fill our desired response.

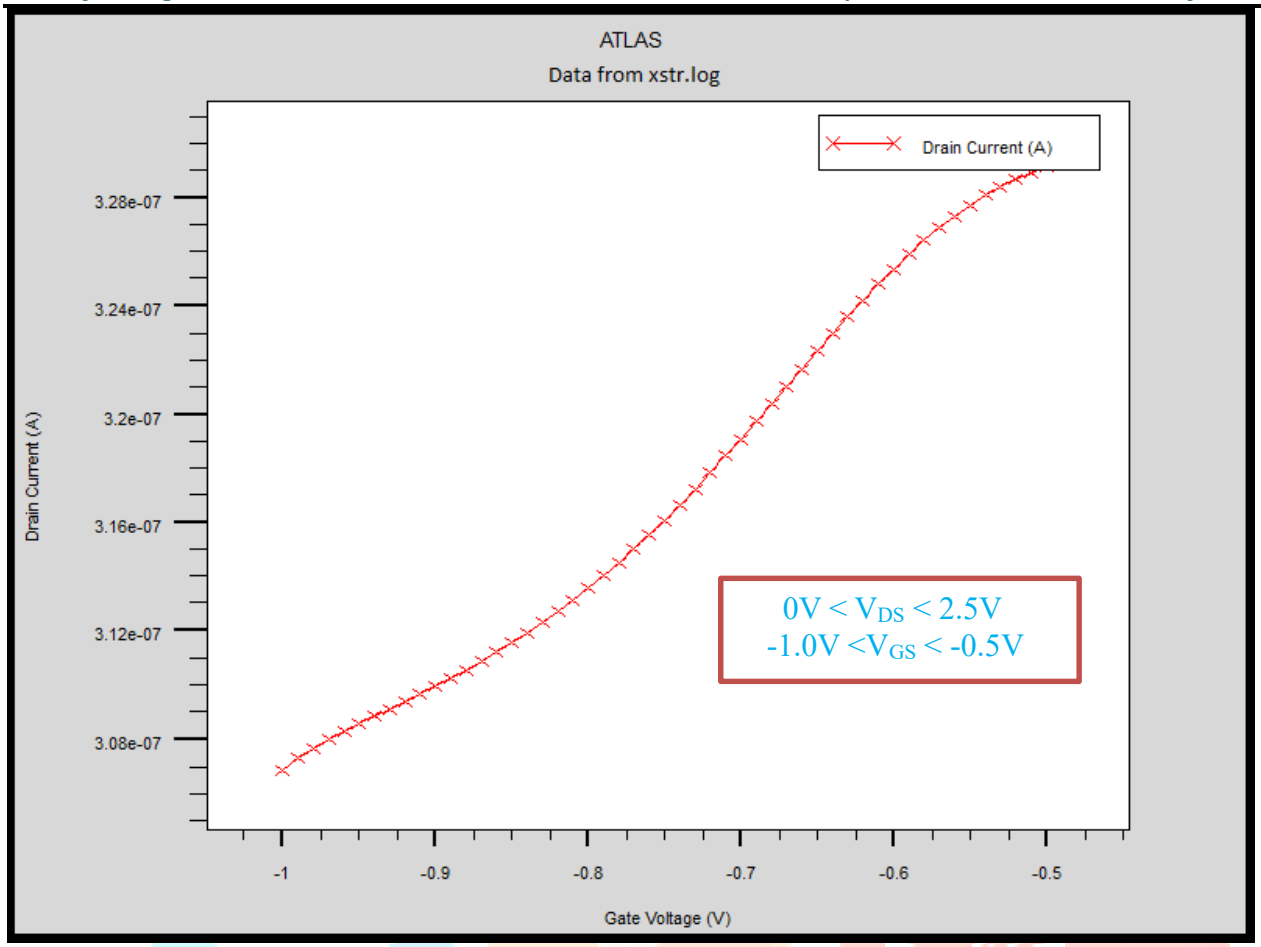

Figure 5-3(a) Drain current (I_D) versus Gate voltage (V_G) without light

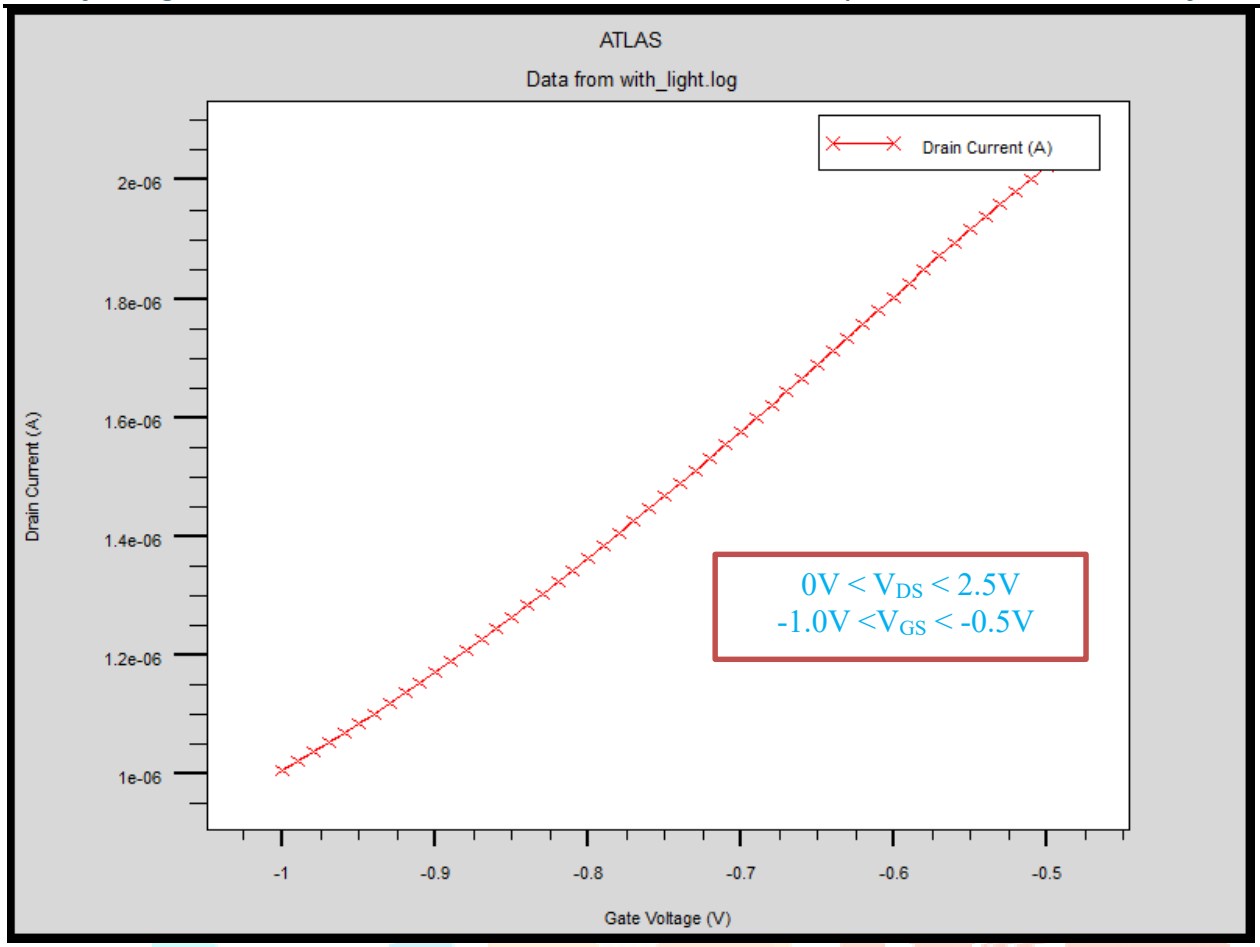

Figure 5-3(b) Drain current (I_D) versus Gate voltage (V_G) with light

.5 Effect of plasmonic layer on the device

In these topics we will see the effect of Plasmon on the surface of the device. This effect is shown in the figure 5.4, in which we added a plasmonic layer of 10nm platinum nanoparticle on the ZnO based Photo-Transistor. The effect of plasmonic is already mentioned in chapter 1. We evaluate all the parameter such as drain characteristics, transfer characteristics, spectral response and responsivity. Now we see the difference between these two i.e. with and without plasmonics. We found that by using plasmonics be get better result than without plasmonics.

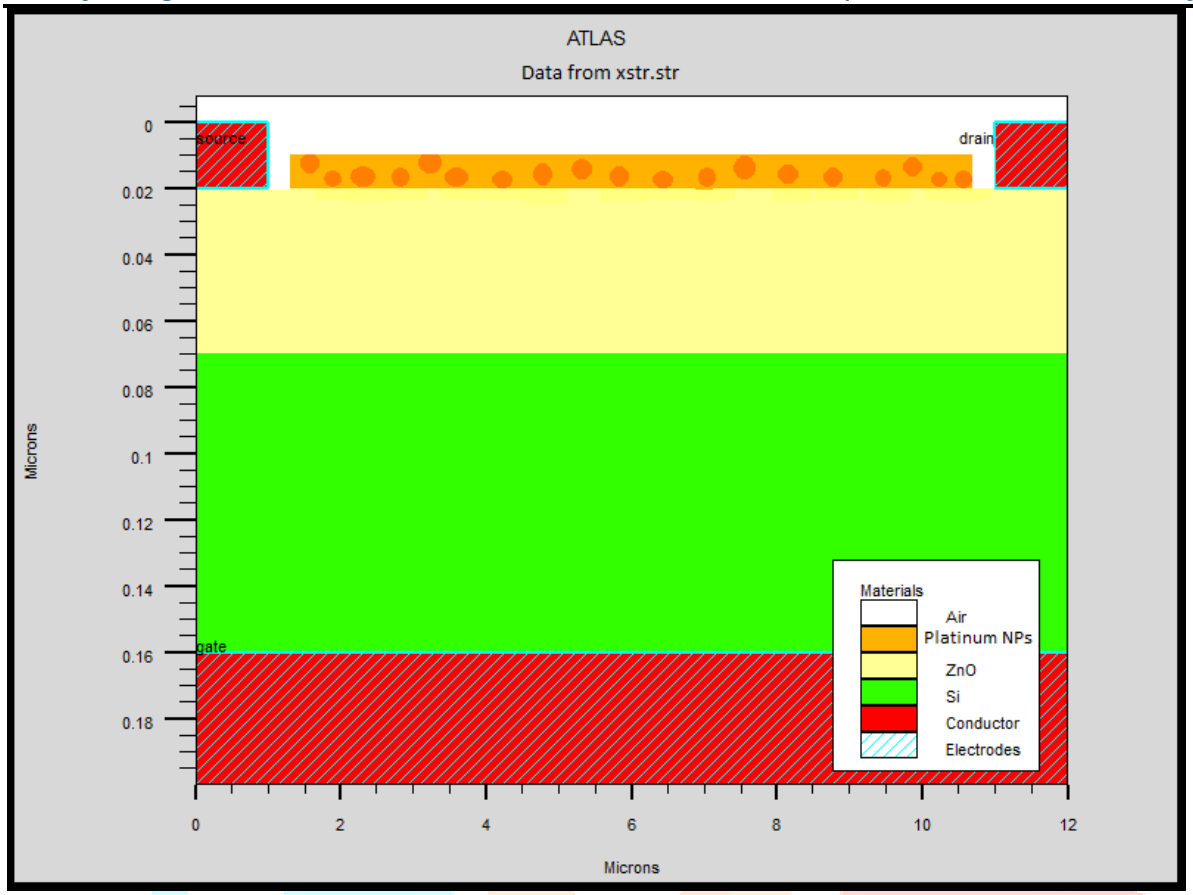

Figure 5-4 Simulated Structure of ZnO based Photo-Transistor with plasmonic

6 Drain Characteristics with plasmonics

Drain characteristics is drawn between drain current and drain voltage. The figure 5.5(a) shows the graph between drain current and drain voltage, in which current is saturated to 3.0×10^{-7}A when we supply drain voltage more than 0.8V.

Now we check the effect of light on the same device under same condition, for this purpose, we incident a beam of light vertical (90°) at the midpoint (6, 0.02) on the device. Beam of light contains a wavelength of 350nm and beam intensity of 550mw/cm^2. After falling the light we found that the current increase approximately 100 times more than the current which are obtained when we not incident light on the device, in this case the drain current increased by increasing the drain voltage and we get max drain current 1.2729×10^{-5}A at drain voltage 2.7V which are shown in figure 5.5(b). Hence we see that by using plasmonics same device will provide better result than previous device in which we not use plasmonic. Hence from the above conclusion we observed that this device full-fill our desired response.

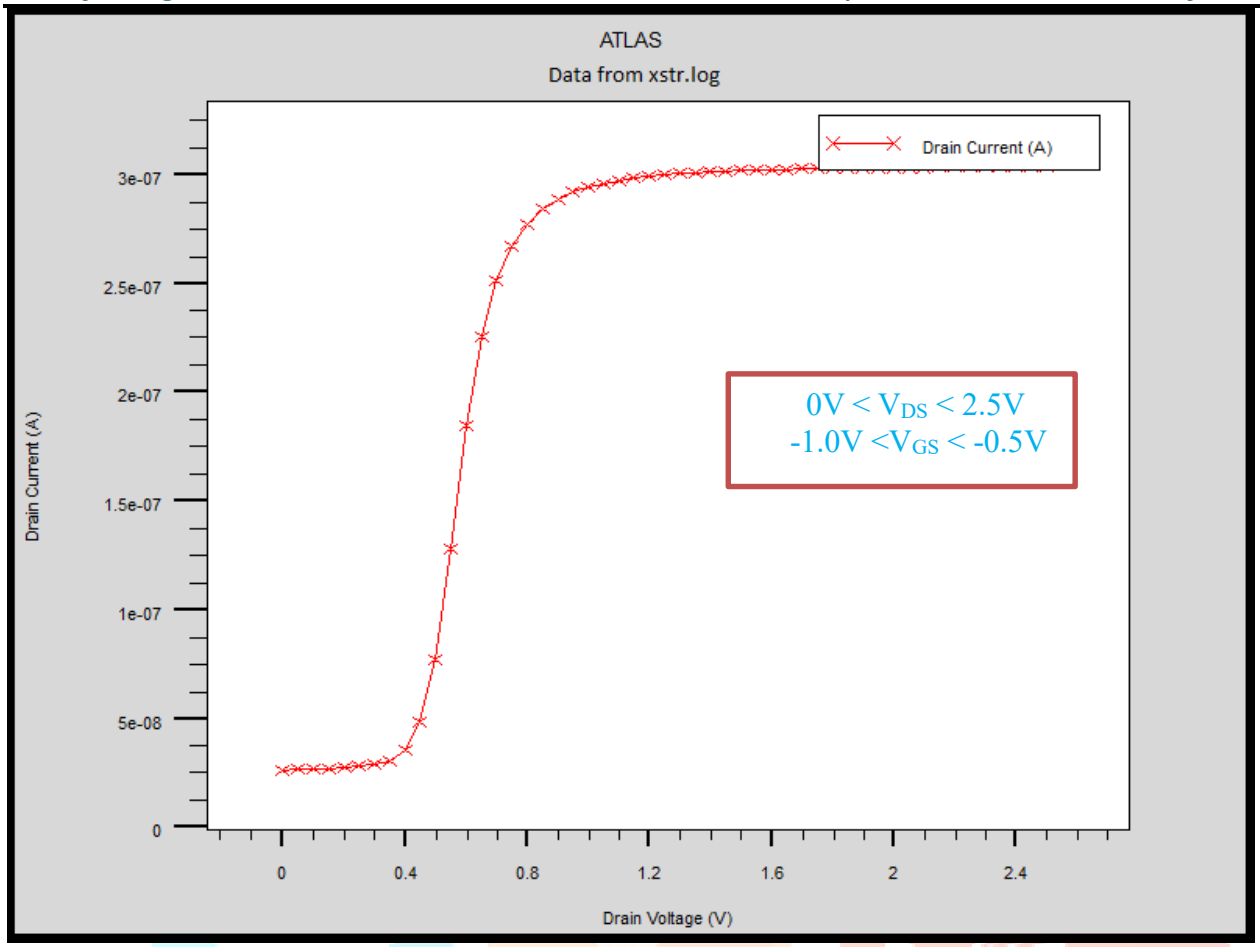

Figure 5-5(a) Drain current (I_D) versus Drain voltage (V_D) without light using plasmonics

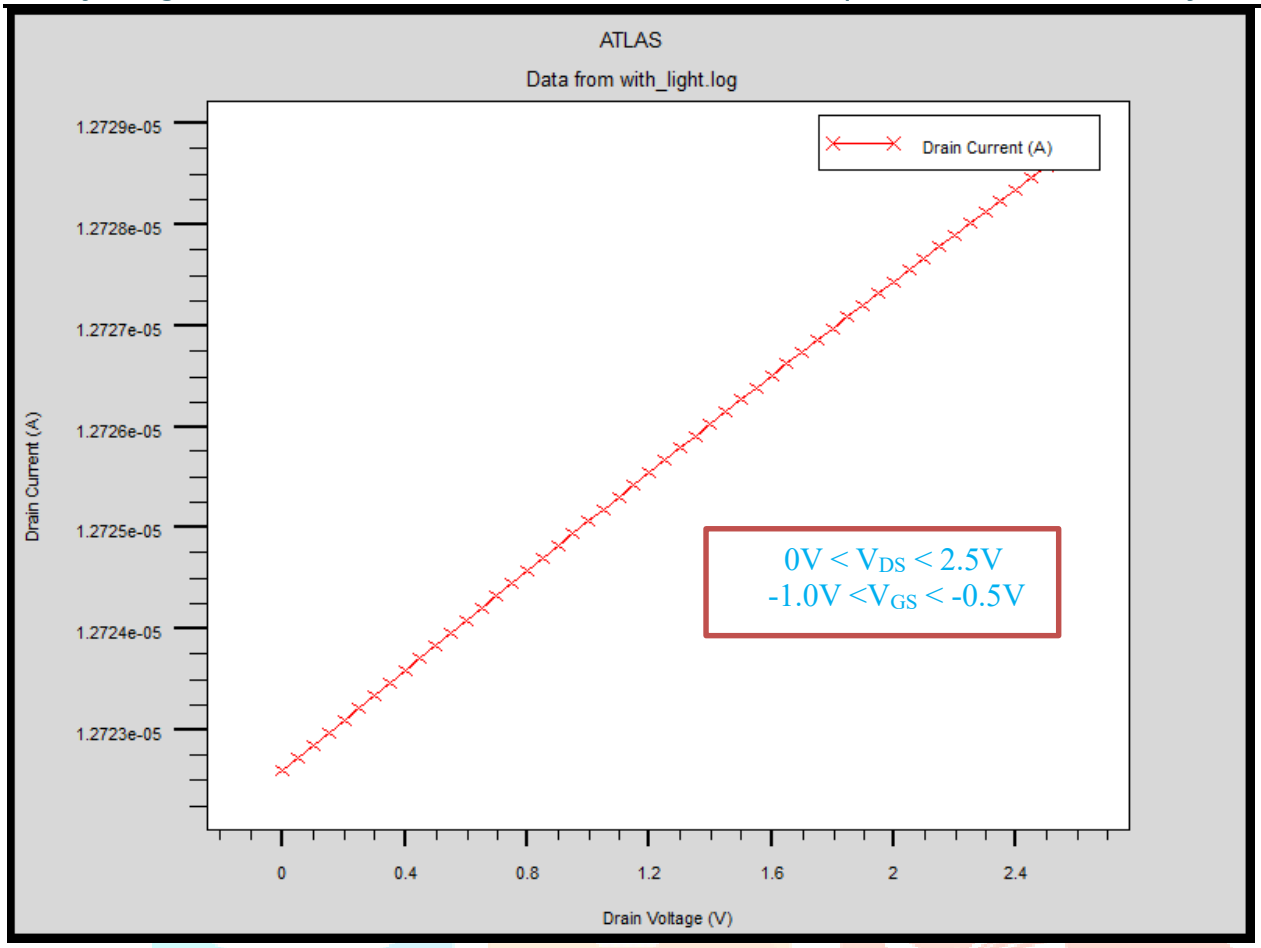

Figure 5-5 (b) Drain current (I_D) versus Drain voltage (V_D) with light using plasmonics

7 Transfer characteristics with plasmonics

Transfer characteristics draw the plot between drain current (I_D) versus gate voltage (V_G).The figure 5.6(a) shown the graph between drain current versus gate voltage, in which drain current decrease with increase in input voltage .The maximum drain current(I_D) is 2.2×10^{-6}A at -1.0 gate voltage(V_G).

Now we check the effect of light on the same device under same condition, for this purpose, we incident a beam of light vertical (90°) at the midpoint (6, 0.02) on the device. Beam of light contains a wavelength of 350nm and beam intensity of 550mw/cm^2. After falling the light we found that the current increase approximately 10 times more than the current which are obtained when we not incident light on the device, in this case the drain current increased linearly with increase in gate voltage and attained a maximum value (1.2722×10^{-5}A) at gate voltage -0.5V which are shown in figure 5.6(b). From the above conclusion we observed that this device full-fill our desired response.

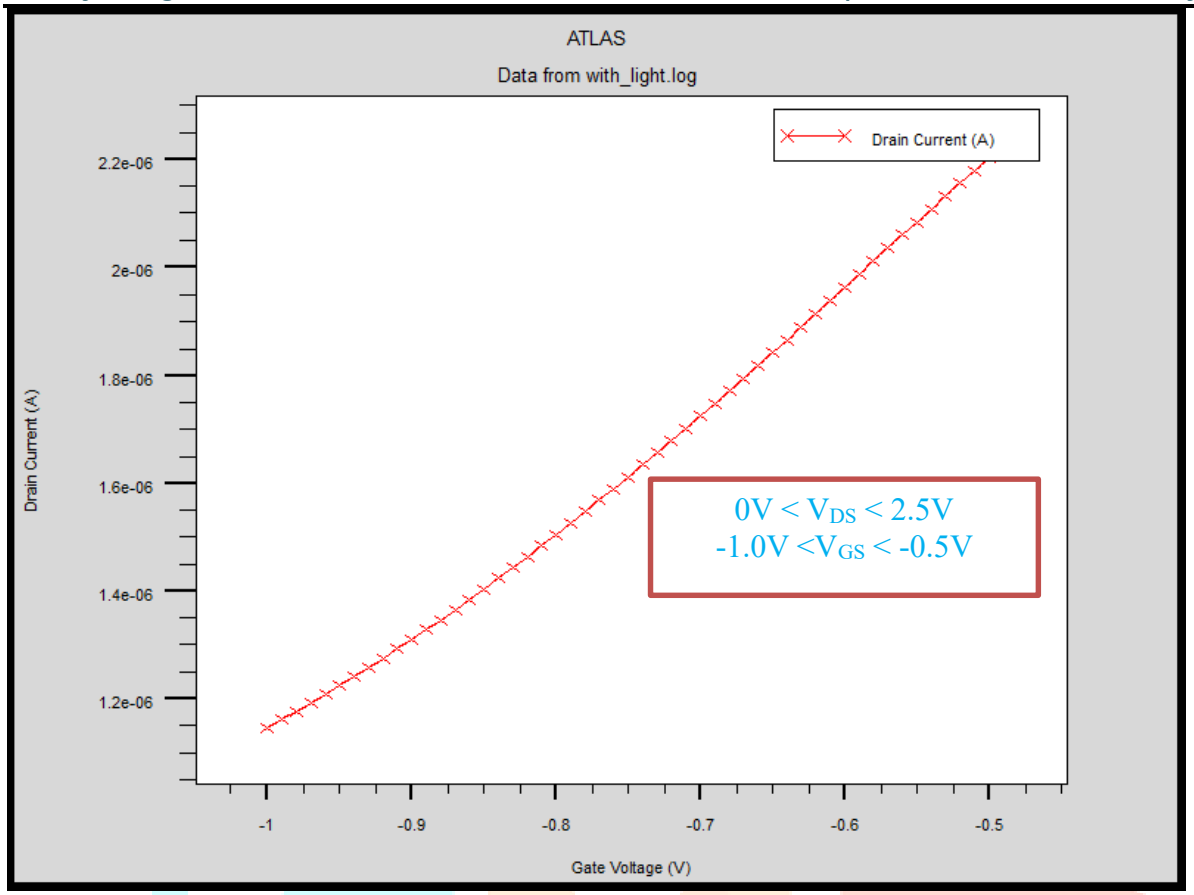

Figure 5-6(a) Drain current (I_D) versus Gate voltage (V_G) without light using plasmonics

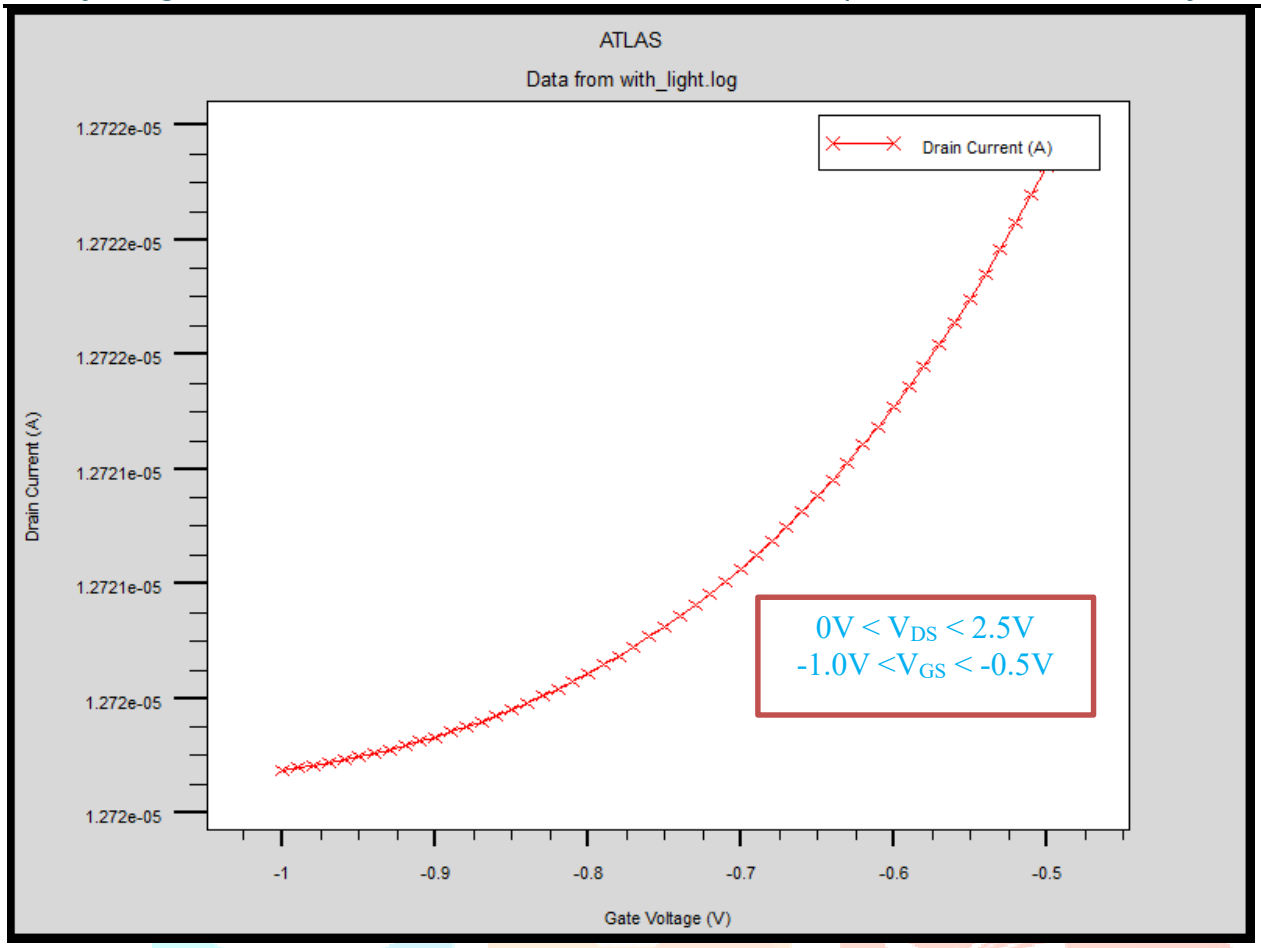

Figure 5-6(b) Drain current (I_D) versus Gate voltage (V_G) with light using plasmonics

8 Spectral responses

In these topics we have to plot a graph between source photo-current versus wavelength, at different value of wavelength (from 200nm to 800nm) with and without plasmonics. Then we compare these two plots, again we found that there is an improvement of spectral response with plasmonics. In figure 5.8(a) we seen that photo current increase from 3×10^{-8}A to 1×10^{-7}A, by increasing the wavelength from 300nm to 1000nm. This source photo-current is obtained when we not using plasmonic on the device .But in figure 5.8(b) we see that source photo current increased by a factor of 100 times ,this is possible due to effect of plasmonic on the device. Hence we observed that 10nm platinum nanoparticles play a very important role in photodetector, because when we not use platinum we found result less than with using platinum.

Since in this simulation we use ZnO as a material hence we can conclude that ZnO is a photo-detecting material.

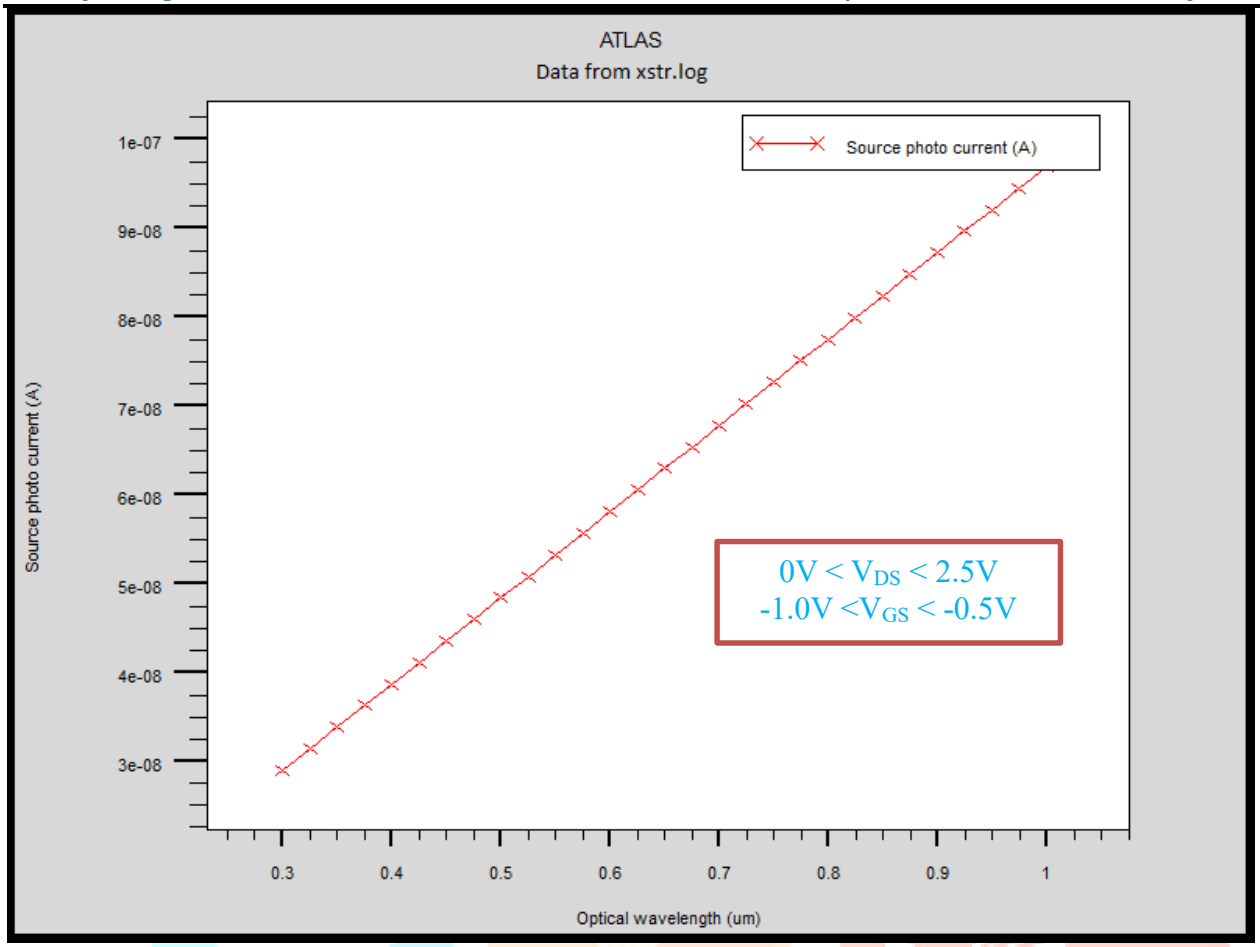

Figure 5-7(a) source photo current versus optical wavelength without plasmonics

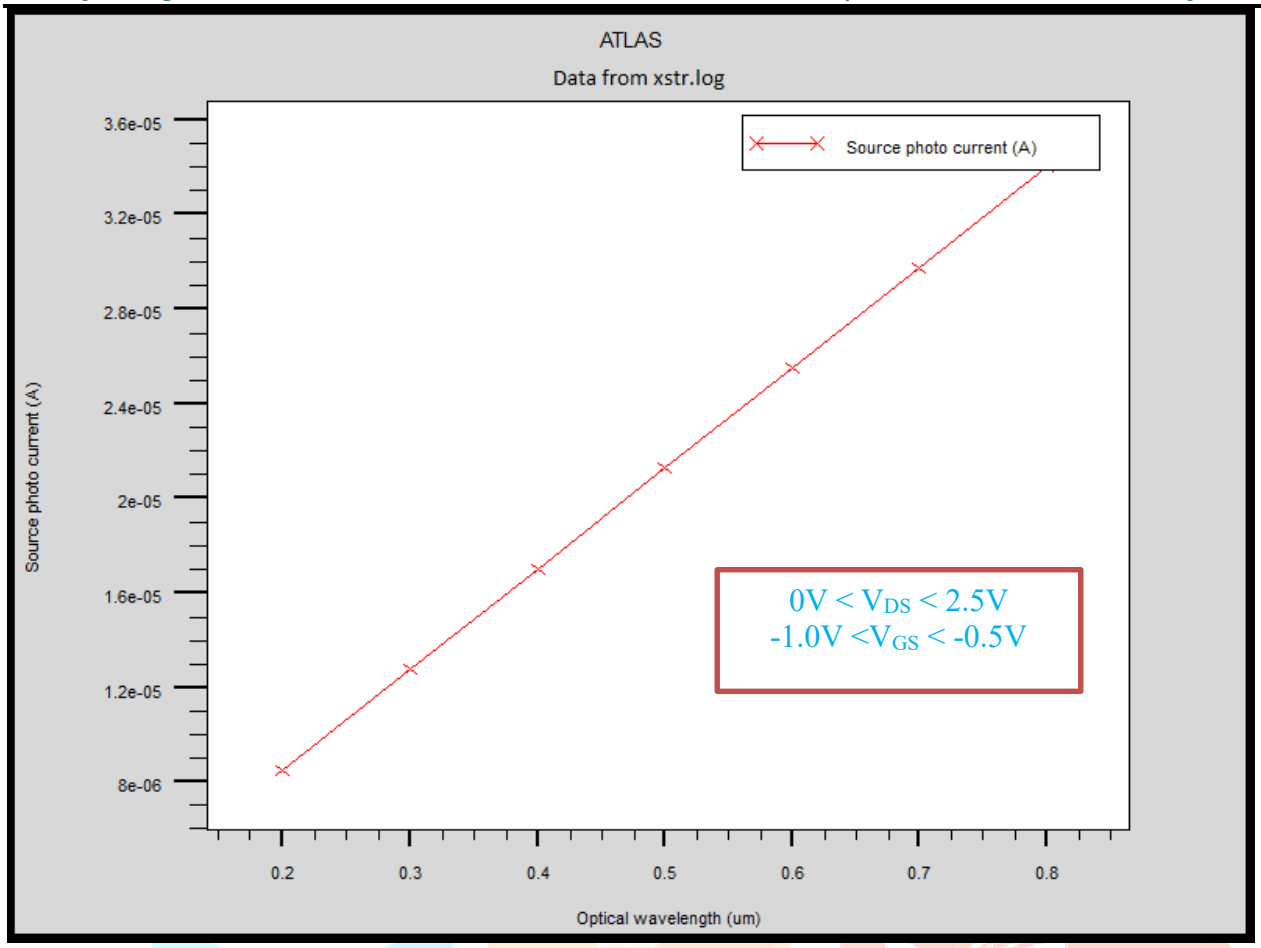

Figure 5-7 (b) source photo current versus optical wavelength with plasmonics

9 Responsivity calculation

Responsivity R_λ is defined as the ratio of radiant energy (in watts),p, incident on the photodiode to the photocurrent output in amperes I_p .It is expressed as the absolute responsivity in amps per watt. Radiant energy is usually expressed as w/cm^2 and that photodiode current as A/cm^2.Responsivity will vary with change in wavelength, bias voltage, and temperature. The responsivity of a photodetector is defined as:

$$R_\lambda = I_{Ph}/P_{opt} = \eta\frac{q\lambda}{hc}$$

Where P_{opt} is the

$$R_\lambda = \frac{I_{ph}}{P_{opt}} = \eta\frac{q\lambda}{hc}$$

h is the plank constant = 6.628×10^{-34} joule-sec

c is the velocity of light in air = 3×10^8 m/s

And I_{ph} is the output photocurrent

Table 5-2 Photo-Detector Responsivity Measurement

Serial number	Responsivity with plasmonics in mA/W	Responsivity without plasmonics in μA/W
1	0.0654	0.18
2	0.0581	0.163
3	0.0509	0.145
4	0.0436	0.127
5	0.0363	0.109
6	0.0290	0.090
7	0.0218	0.072
8	0.0145	0.054

Table 5.2 is obtained by using above formula, in which we use optical power intensity is 550mW/cm^2 .We have already seen photo current with and without plasmonic in figure 5.8(a) and 5.8(b) respectively. Hence by the help of these two, we evaluate the value of responsivity. We also calculate the value of responsivity by the help of efficiency of internal quantum efficiency.

CHAPTER 6

6 CONCLUSION & FUTURE SCOPE

6.1 Conclusion

The optical and electrical properties of ZnO play a very important role for various device applications such as UV photodetectors, LEDs, lasers and TFTs. In this project work, I have simulated ZnO based UV Photo-Transistor with plasmonics enhancement by using Atlas software. The platinum (metal) nanoparticles are coated on the surface of the device.

Based on the result obtained, we conclude that the ZnO based UV Photo-Transistor has a total drain saturation current of 1.708×10^{-7}A .Now when we incident light of wavelength 350nm the drain saturation current increased up to 10 times which is equal to 1.748×10^{-6}A. Hence we can conclude that ZnO is a photo detecting material.

This performance can be further increased by using platinum nanoparticles for plasmonic enhancement of drain current. It was observed that the plasmonic layer enhanced the drain saturation current by a factor of 100 i.e. Drain saturation current without light is 3.048×10^{-7}A and with light is 1.2755×10^{-5}A.

Also the maximum responsitivity of the devices was found to be 0.0654mA/W and 0.18μA/W with and without plasmonic layer. The values obtained in the simulation are closed to the values quoted in the literature [62-82].Hence according to our study the platinum nanoparticles play a key role in enhancing the performance of photodetectors.

.2 FUTURE SCOPE

In this dissertation simulation studies of ZnO based UV Photo-Transistor with and without plasmonic enhancement have done, but still there are some complicated issues which can be taken care of as future work. Hence the simulation of P-type ZNO-based material can also be studies

We also perform the analysis of ZnO based Ultraviolet photodetector Thin Film Transistor in which sio_2 is used as dielectric materials, which separate metal and semiconductor. Since my project is quiet similar to this because instead of sio_2 we use p-Type silicon which will operates when we supply negative gate voltage.

Some more studies like variation of UV current with temperature ,study related to gas sensing have not been considered in this dissertation, these studies may also be consider in future work.

This project can also help in simulation studies of ZnO based UV MSM Photodetector(PD),which is possible when (1)we will remove gate terminal from the above mentioned structures and (2)instead of P-type silicon substrate we simply use silicon as a substrate

The observed results provide an indication that the plasmonic assisted UV response of the novel metal ZnO photo-transistor might provide a breakthrough for the development of next generation photodetectors.

APPENDIX

DEVICE SIMULATION CODE

```
go atlas
mesh space.multi=.5
x.mesh   loc=0.       spac=.1
x.mesh   loc=1        spac=0.1
x.mesh   loc=11       spac=0.1
x.mesh   loc=12       spac=0.1
y.mesh   loc=0        spac=0.005
#y.mesh loc=0.015  spac=0.001
y.mesh   loc=0.02     spac=0.001
y.mesh   loc=0.07     spac=.002
y.mesh   loc=0.12     spac=0.005
y.mesh   loc=0.20     spac=0.005

region num=1    x.min=0   x.max=12   y.min=0.0    y.max=0.20    material=Air
region num=2    x.min=2   x.max=10   y.min=0.01   y.max=0.02    material=platinum
region num=3    x.min=0   x.max=12   y.min=0.02   y.max=0.07    material=Zno
region num=4    x.min=0   x.max=12   y.min=0.07   y.max=0.16    material=si
#region num=4  x.min=0   x.max=12   y.min=0.16   y.max=0.20    material=Titanium

electrode   name=source         number=1  x.min=0   x.max=1    y.min=0       y.max=0.02
electrode   name=drain          number=2  x.min=11  x.max=12   y.min=0       y.max=0.02
electrode   name=gate           number=3 x.min=0    x.max=12   y.min=0.16    y.max=0.20
electrode   name=conductor      number=4  x.min=1    x.max=11   y.min=0.01    y.max=0.02
#
contact    name=source     workfunction=5.1
contact    name=drain      workfunction=5.1
contact    name=gate       workfunction=4.6

doping region=1  x.min=0  x.max=12  y.min=0.07  y.max=0.16   p.type conc=1e15 uniform
doping region=2  x.min=0  x.max=12  y.min=0.02  y.max=0.07   n.type conc=1e17 uniform

material name=ZnO  eg300=3.37  mun=60  mup=10  permittivity=8.5 \
nc300=2.94E24  nv300=1.13E25  affinity=4.3  m.vthn=0.19  m.vthp=1.21\

models  fermidirac  consrh cvt  bgn auger ni.fermi
 material taup0=2.e-6 taun0=2.e-6

#model srh cvt conmob fldmob
save outf=xstr.str
tonyplot xstr.str
```

```
#method newton
method  newton carrier=2 trap itlimit=25 atrap=0.5 maxtraps=4\autonr nrcriterion =0.1 tol.time=0.005 dt.min=1e-25 method newton trap

solve init
solve vdrain=0.1
solve vdrain=0.2
solve vdrain=0.3
solve vgate=-0.5 vstep=-0.01 vfinal=-1.0 name=gate
log outf=xstr.log
solve vdrain=0.0 vstep=0.05 vfinal=2.5 name=drain

output e.field recombination band.param con.band val.band e.mobility ex.velocity \
ey.velocity e.velocity impact.i flowlines charge j.drift j.total j.diffusion

save outf=xstr.str
tonyplot xstr.log  xstr.str
log off
# Optical source definition

# define a ultraviolet light  normal to top (y=0.02) surface
# this beam is as follows:
#beam #1, originating at (6.0, 0.02), propagating at an angle of 90 degrees, with a    ultraviolet light


#beam num=1 x.origin=6.0 y.origin=0.02 beam width=.2 angle=90.0 wavelength=350nm
solve init
beam num=1 wavelength=.350 x.ori=6.0 y.ori=0.02 max.win=.2 angle=90
solve vdrain=0.1
solve vdrain=0.2
solve vdrain=0.3

solve vgate=-0.5 vstep=-0.01 vfinal=-1.0 name=gate

solve vdrain=0.0
solve b1=550 beam=1
#solve b1=0 ramp.lit
log outf=with_light.log
solve   vdrain=0.0 vstep=0.05 vfinal=2.5 name=drain
#solve vdrain=0.0 vstep=0.05 vfinal=2.5 name=gate beam num=1
```

Appendix

```
log off
tonyplot xstr.str
tonyplot xstr.log with_light.log
##############
solve init
beam num=1 wavelength=.1 x.ori=6.0 y.ori=0.02 max.win=.2 angle=90
#
method newton trap
solve init
solve vdrain=0.1
solve vdrain=0.2
solve vdrain=0.3
solve vgate=-0.5 vstep=-0.01 vfinal=-1.0 name=gate
log outf=xstr .log
solve vdrain=0.0 vstep=0.05 vfinal=2.5 name=drain

# SECTION 5: Spectral Response
#
log outf=xstr.log master
solve prev b1=550 lambda=0.2
solve prev b1=550 lambda=0.3
solve prev b1=550 lambda=0.4
solve prev b1=550 lambda=0.5
solve prev b1=550 lambda=0.6
solve prev b1=550 lambda=0.7
solve prev b1=550 lambda=0.8

tonyplot  xstr.log -set xstr.set
quit
```

REFERENCES

[1] Daniel, M.-C; Astruc, D. Chemical Reviews 2003,104, 293.

[2] Trindade, T.; O'Brien, P.; Pickett, N. L. Chemistry of Materials 2001, 13, 3843.

[3] Lin, C.H., Liu, C.W. Metal-insulator-semiconductor photodetectors. Sensors2010, 10, 8797– 8826.

[4] Monroy, E.; Omnes, F.; Calle, F. Wide-bandgap semiconductor ultraviolet photodetectors. Semicond. Sci. Technol. 2003, 18, R33–R51.

[5] Omnes, F. Monroy, E., Munoz, E.; Reverchon, J. L., "Wide bandgap UV photodetectors: A short review of devices and applications" Proc. SPIE 2007, 6473E, pp. 1–15.

[6] Lee, Y. K.; Jung, C. H.; Park, J.; Seo, H.; Somorjai, G. A.; Park, J. Y. Nano Lett. 2011, 11 (10),pp 4251−4255.

[7] Mubeen, S.; Hernandez-Sosa, G.; Moses, D.; Lee, J.; Moskovits, M. Nano Lett. 2011, 11 (12), 5548−5552.

[8] Wang, F.; Melosh, N. A. Nano Lett. 2011, 11 (12), 5426−5430.

[9] Chen, J.; Badioli, M.; Alonso-Gonzalez, P.; Thongrattanasiri, S.; Huth, F.; Osmond, J.; Spasenovic, M.; Centeno, A.; Pesquera, A.; Godignon, P.; Zurutuza Elorza, A.; Camara, N.; de Abajo, F. J. G.; Hillenbrand, R.; Koppens, F. H. L. Nature 2012, 487 (7405), 77−81.

[10] Fang, Z.; Wang, Y.; Liu, Z.; Schlather, A.; Ajayan, P. M.; Koppens, F. H.; Nordlander, P.; Halas, N. J. ACS Nano 2012, 6 (11), 10222−10228

[11] Q.A. Xu, J.W. Zhang, K.R. Ju, X.D. Yang, X. Hou, ZnO thin film photoconductive ultraviolet detector with fast photoresponse, J. Cryst. Growth 289 (2006) 44.

[12] Yang, H.M., Park, C.W., Ahm, T., Jung, B., Seo, B., Park, H., Kim, J.D., 2013. A direct surface modification of iron oxide nanoparticles with various poly (amino acid)s for use as magnetic resonance probes, Journal of Colloid and Interface Science, 1;391: 158-167.

[13] R. Shrivastava, "Fundamentals of electronic devices", Krishna Prakashan Media, pp. 173-175, 2009.

[14] P. K. Weimer, "TFT – new thin-film transistor" , Proceedings of the Institute of Radio Engineers, vol. 50, pp. 1462-1469, 1962.

[15] A. T. Voutsas and M. K. Hatalis, "Technology of polysilicon thin-film transistors", in "Thin-film transistors", ed. C. R. Kagan and P. Andry, Marcel Dekker Incorporated, pp. 149-168, 2003.

[16] R. L. Hoffman, B. J. Norris, and J. F. Wager, "ZnO-based transparent thin-film transistors", Applied Physics Letters, vol. 82, issue 5, pp. 733-735, 2003.

[17] E. Fortunato, P. Barquinha, A. Pimentel, A. Gonçalves, A. Marques, L. Pereira, and R. Martins, "Zinc oxide thin-film transistors", in "Zinc oxide – a material for micro- and optoelectronic applications", ed. N. H. Nickel and E. Terukov, vol. 194, Springer, pp. 225-237, 2005.

[18] R. L. Hoffman, B. J. Norris and J. F. Wager, "ZnO-based transparent thin-film transistors",Appl. Phys. Lett., Vol. 82, No. 5, 3 February 2003

19] S. J. Pearton, D. P. Norton, K. Ip, Y.W. Heo, T. Steiner," Recent progress in processing and properties of ZnO" Prog. in Mat. Sci., 50 (2005) 293-295.

20] S. Singh, P. Thiyagarajan, K. M. Kant, D. Anita, S. Thirupathiah, N. Rama, B. Tiwari, M. Kottaisamy and M. S. R. Rao, "Structure, microstructure and physical properties of ZnO based materials in various forms: bulk, thin film and nano" J. of Phys. D: Appl. Phy., 40, (2007) 6312-6316.

21] S. Singh and P. Chakrabarti, "Simulation, Fabrication and Characterization of ZnO Based Thin Film Transistors Grown by Radio Frequency Magnetron Sputtering" J. of Nanosci. &Nanotech., 12, (2012) 1880-1885.

22] M.F.A. Alias, H.Kh. Alamy and R.M. Aljarrah, "The Role of Thickness on the Structural and Electrical Properties of Dc Magnetron Sputtered Nano Zno Thin Films," J. Elec. Dev., 14 (2012) 1178-1185.

23] F. Chowdhury, "Influence of Thickness Variation on the Optical Properties of ZnO thin films prepared by thermal evaporation method," J. Elec. Dev.,10 (2011) 448-455.

24] S. Rajesh1, T. Ganesh2 and Francis P. Xavier, "Thickness dependent microstructure, optical and photo conducting properties of ZnO thin films prepared by spin coating process," J. Elec. Dev., 17 (2013) 1417-1422

25] F. Chowdhury, "Influence of Thickness Variation on the Optical Properties of ZnO thin films prepared by thermal evaporation method," J. Elec. Dev.,10 (2011) 448-455.

26] S. Rajesh1, T. Ganesh2 and Francis P. Xavier, "Thickness dependent microstructure, optical and photo conducting properties of ZnO thin films prepared by spin coating process," J. Elec. Dev., 17 (2013) 1417-1422

27] E. FortunatoT, P. Barquinha, A. Pimentel, A. Gonc¸alves, A. Marques, L. Pereira, R. Martins, "Recent advances in ZnO TFTs" Thin Solid Films 487, (2005) 205.

28] T. Hirao, M. Furuta, H. Furuta, and T. Matsuda, T. Hiramatsu, H. Hokari, M. Yoshida, H. Ishii and M. Kakegawa, "Bottom-Gate Zinc Oxide Thin-Film Transistors (ZnO TFTs) for AM-LCDs" J. Soc. Inf. Display 15, (2007) 17.

29] R. L. Hoffman, "ZnO-channel thin-film transistors: Channel mobility" J. Appl. Phys. 95, (2004) 5813.

30] E.M.C. Fortunato, P.M.C. Barquinha, A.C.M.B.G. Pimentel, A.M.F. Gonvalves, "Wide-bandgap high-mobility ZnO thin-film transistors produced at room temperature" Appl. Phys. Lett. 85, (2004) 2541.

31] T.I. Suzuki, A. Ohtomo, A. Tsukazaki, F. Sato, J. Nishii, H. Ohno, M. Kawasaki, "Hall and Field-Effect Mobilities of Electrons Accumulated at a Lattice-Matched ZnO/ScAlMgO4 Heterointerface"Adv.Mater. 16, (2004) 1887.

32 P. K. Shin, Y. Aya, T. Ikegami, K. Ebihara, "Application of pulsed laser deposited zinc oxide films to thin film transistor device" Thin Solid Films 516, (2008) 3767.

33] S. Sriram and A. Thayumanavan, "Optical and electrical properties of nitrogen doped ZnO thin films prepared by low cost spray pyrolysis technique," J. Elec. Dev., 15, (2012) 1215-1224.

[34] S. Singh and P. Chakrabarti, "Simulation, Fabrication and Characterization of Sol–Gel Deposited ZnO Based Thin Film Transistors," Sci. Adv. Mat. 4 (2012) 199–203.

[35] S. Singh and P. Chakrabarti, "Simulation, Fabrication and Characterization of Sol–Gel Deposited ZnO Based Thin Film Transistors," Sci. Adv. Mat. 4 (2012) 199–203.

[36] H. C. Cheng, C. F. Chen, C. C. Lee, "Thin-film transistors with active layers of zinc oxide (ZnO) fabricated by low-temperature chemical bath method" Thin Solid Films 498, (2006) 142.

[37] H. Fabricius, T. Skettrup, P. Bisgaard Appl. Opt., 25 (1986), p. 2764 CrossRefView Record in Scopus

[38] C.H. Park, I.-S. Jeong, J.H. Kim, S. Im Appl. Phys. Lett., 83 (2003), p. 2946

[39] Monroy E, Calle F, Pau JL, Munoz E, Omnes F, Beaumont B, Gibart P. AlGaN-Based UV Photodetectors. J. Cryst. Growth. 2001;230:537–543.

[40] Munoz E, Monroy E, Pau JL, Calle F, Omnes F, Gibart P., III Nitrides and UV Detection. J. Phys.: Condens. Matter. 2001;13:7115–7137.

[41] Chiou YZ, Tang JJ. GaN Photodetectors with Transparent Indium Tin Oxide Electrodes. JPN. J. Appl. Phys. 2004;43:4146–4149.

[42] Ozgür Ü, Alivov YA, Liu C, Teke A, Reshchikov MA, Dogan S, Avrutin V, Cho SJ, Morkoç H. A Comprehensive Review of ZnO Materials and Devices. J. Appl. Phys. 2005;98:041301

[43] Pearton SJ, Norton DP, Ip K, Heo YW, Steiner T. Recent Advances in Processing of ZnO. J. Vac. Sci. Technol. B. 2004;22:932–948.

[44] Look DC. Recent Advances in ZnO Materials and Devices. Mater. Sci. Eng. B. 2001;80:383–387.

[45] Ohtomo A, Kawasaki M, Sakurai Y, Yoshida Y, Koinuma H, Yu P, Tang ZK, Wong GKL, Segawa Y. Room Temperature Ultraviolet Laser Emission From ZnO Nanocrystal Thin Films Grown by Laser MBE. Mater. Sci. Eng. B. 1998;54:24–28.

[46] Gruber Th, Kirchner C, Kling R, Reuss F, Waag A. ZnMgO Epilayers and ZnO-ZnMgO Quantum Wells for Optoelectronic Applications in the Blue and UV Spectral Region. Appl. Phys. Letts. 2004;84:5359–5361.

[47] Mollow E. In: Proceedings of the Photoconductivity Conference. Breckenridge RG, editor. Wiley; New York, NY, USA: 1954. p. 509.

[48] Fabricius H, Skettrup T, Bisgaard P. Ultraviolet Detectors in Thin Sputtered ZnO Films. Appl. Opt. 1986;25:2764–2767. [PubMed]

[49] Zhai T, Fang X, Liao M, Xu X, Zeng H, Bando Y, Golberg D. A Comprehensive Review of One-Dimensional Metal-Oxide Nanostructure Photodetectors. Sensors. 2009;9:6504–6529. [PMC free article][PubMed]

[50] Shen G, Chen D. One-Dimensional Nanostructures for Photodetectors. Recent Patente Nanotechnol. 2010;4:20–31. [PubMed]

[51] Hahn, E. E. J. Appl. Phys. 1951, 22, 855−863.

[52] Melnick, D. A. J. Chem. Phys. 1957, 26, 1136−1146.

53] Razeghi, M.; Rogalski, A. J. Appl. Phys. 1996, 79, 7433−7473.

54] Liu, K. W.; Sakurai, M.; Aono, M. Sensors 2010, 10, 8604−8634.

55] Moazzami, K.; Murphy, T. E.; Phillips, J. D.; Cheung, M. C. K.; Cartwright, A. N. Semicond. Sci. Technol. 2006, 21, 717−723.

56] Liu, M. J.; Kim, H. K. Appl. Phys. Lett. 2004, 84, 173−175.

57] Zhang, D. H. J. Phys. D: Appl. Phys. 1995, 28, 1273−1278.

58] Kumar, S.; Gupta, V.; Sreenivas, K. Nanotechnology 2005, 16, 1167−1171.

59] Liang, S.; Sheng, H.; Liu, Y.; Huo, Z.; Lu, Y.; Shen, H. J. Cryst. Growth 2001, 225, 110−113.

60] Sarkar, K.; Rawolle, M.; Herzig, E. M.; Wang, W. J.; Buffet, A.; Roth, S. V.; Muller-Buschbaum, P. Chem. Sus. Chem. 2013, 6, 1414−1424.

61] Chen, Y.; Ko, H. J.; Hong, S. K.; Yao, T. Appl. Phys. Lett. 2000, 76, 559−561.

62] Xue, S. W.; Zu, X. T.; Zhou, W. L.; Deng, H. X.; Xiang, X.; Zhang, L.; Deng, H. J. Alloys Compd. 2008, 448, 21−26.

63] Li, M.; Anderson, W.; Chokshi, N.; Deleon, R. L.; Tompa, G. J. Appl. Phys. 2006, 100, 053106.

64] Bang, K. H.; Hwang, D. K.; Myoung, J. M. Appl. Surf. Sci. 2003, 207, 359−364.

65] Tsukazaki, A.; Ohtomo, A.; Yoshida, S.; Kawasaki, M.; Chia, C. H.; Makino, T.; Segawa, Y.; Koida, T.; Chichibu, S. F.; Koinuma, H. Appl. Phys. Lett. 2003, 83, 2784−2786.

66] Suvorova, N. A.; Usov, I. O.; Stan, L.; DePaula, R. F.; Dattelbaum, A. M.; Jia, Q. X.; Suvorova, A. A. Appl. Phys. Lett. 2008, 92, 141911.

67] Ali, G. M.; Chakrabarti, P. Appl. Phys. Lett. 2010, 97, 031116.

68] Kwon, M. K.; Kin, J. Y.; Kim, B. H.; Park, I. K.; Cho, C. Y.; Byeon, C. C.; Park, S. J. Adv. Mater. 2008, 20, 1253−1257.

69] You, J. B.; Zhang, X. W.; Zhang, S. G.; Yin, Z. G.; Wang, J. X.; Yin, Z. G.; Tan, H. R.; Zhang, W. J.; Chu, P. K.; Cui, B.; Wowchak, A. M.; Dabiran, A. M.; Chow, P. P. Appl. Phys. Lett. 2010, 96, 201102.

70] Dufaux, T.; Dorfmuller, J.; Vogelgesang, R.; Burghard, M.; Kern, K. Appl. Phys. Lett. 2010, 97, 161110.

71] Li, J.; Ong, H. C. Appl. Phys. Lett. 2008, 92, 121107

72] S. M. Sze. Semiconductor Devices, Physics and Technology. 2nd edition, Wiley.

73] G. F. Knoll. Radiation Detection and Measurement. 4th edition, Wiley.

74] W.R.LEO and D.Neamen.